

Origin of step-like and lobate seafloor features along the continental shelf off Rio de Janeiro State, Santos basin-Brazil

A.T. Reis^{a,*}, R.M.C. Maia^b, C.G. Silva^b, M. Rabineau^c, J.V. Guerra^a, C. Gorini^d, A. Ayres^b,
R. Arantes-Oliveira^a, M. Benabdellouahed^e, I. Simões^f, R. Tardin^a

^a Departamento de Oceanografia Geológica, Faculdade de Oceanografia, Universidade do Estado do Rio de Janeiro (UERJ), Rua São Francisco Xavier, 524, Maracanã, CEP 20.550-900 Rio de Janeiro/RJ, Brazil

^b Departamento de Geologia/LAGEMAR, Instituto de Geociências, Universidade Federal Fluminense (UFF), Av. Gen. Milton Tavares de Souza, s/no. 4° andar, Campus da Praia Vermelha, Gragoatá, CEP 24210-346 Niterói/RJ, Brazil

^c CNRS, Domaines Océaniques (UMR6538), Equipe Transferts Terre-Mer, Institut Universitaire des Sciences de la Mer (IUEM), Université de Bretagne Occidentale (UBO), 1, Place N. Copernic, Plouzané 29280, France

^d Laboratoire Evolution et Modélisation des Bassins Sédimentaires, Institut de Science de la Terre-ISTEP (UMR CNRS 7193), Université Pierre et Marie Curie-Paris 6, 4 Place Jussieu, 75005 Paris, France

^e Ifremer Centre de Brest, DRO/Géosciences Marines, B.P. 70, 29280 Plouzané Cedex, France

^f Instituto de Estudos do Mar Almirante Paulo Moreira (IEAPM), Praça Daniel Barreto s/no., Praia dos Anjos, CEP 28.930-000 Arraial do Cabo/RJ, Brazil

*: Corresponding author : A. T. Reis, email address : antonio.tadeu@pq.cnpq.br

Abstract:

A combined analysis of seismic and morphological features identified in a set of high-resolution seismic reflection and bathymetric data, shows a systematic relationship between major modern seafloor morphological traces and the basinward migration of Late Pleistocene coastlines along the continental shelf of the Santos basin (Rio de Janeiro State, SE Brazil). Observed fairly continuous and sinuous mid-outer shelf escarpments are related to the sea-level variations and shelf exposure during the Last Glacial cycle. A bathymetric step at – 110 m is an erosional remnant of offlapping detached forced-regressive wedges that spread over 50 km in the shelf-dip direction, probably developed during periods of falling sea level between MIS 3 and 2. A second major escarpment at – 130 m was interpreted as the shoreline during the LGM, at the time of most extensive subaerial exposure of the continental shelf. However, a distal escarpment at – 150 m is expressed as a straight contour feature along the two main shelf-edge embayments that characterize the shelf break. This escarpment is coupled with a basal seaward-inclined and highly eroded ramp, and was interpreted as the erosional action of bottom currents during the last transgression due to the displacement of the southward flowing Brazil Current towards the present-day outer shelf. Previously published articles have regarded the morphological features observed on the modern shelf as indicators of stillstands during the post-LGM transgression. We conclude that, on the contrary, most of these features are actually from earlier parts of the Late Pleistocene and were formed in a regressive scenario under oscillating and relative slow sea-level fall.

Highlights

► Geomorphologic indicators of Latest Quaternary sea-level oscillations ► Drowned outer shelf deposits related to stepped forced-regressive wedges ► Linear bathymetric steps formed during the Late Pleistocene sea level regression ► Last Glacial Maximum shoreline preserved at 130 m below modern sea level ► Escarpment at – 150 m sculpted by the southward flowing Brazil Current

Keywords: Continental shelf geomorphology ; Forced regression ; LGM shoreline ; Late Pleistocene ; Post-LGM transgression ; Brazil Current

1. Introduction

Drowned Late Pleistocene–Early Holocene features remain poorly documented on the continental shelf off southern Rio de Janeiro State (referred to hereafter as RJ; Fig. 1), in the northern Santos basin, as well as on the entire Brazilian continental margin as a whole. In this context, high resolution seismic stratigraphic studies may provide valuable information for the understanding of the glacio-eustatic meaning of subsurface shelf architecture and surface shelf morphology. However, until recently, the geomorphological evolution of drowned seabed features observed on the southern RJ shelf had been investigated only through the examination of conventional bathymetric survey data. A few pioneer studies carried out in the 1970s and 1980s (Zembruscki, 1979, Corrêa et al., 1980 and Costa et al., 1988) interpreted the origin of a series of continuous linear step-like

63 seabed features as the geomorphic indicators of palaeoshorelines (beach sand
64 ridges) developed during successive stages of sea-level stillstand around the
65 present-day 25, 32, 50, 60, 90 and 110-m isobaths, in the course of the latest
66 Pleistocene-Holocene transgression, while a continuous escarpment located at
67 –130 m was correlated to shoreface features related to the Last Glacial Maximum
68 (LGM) (Costa et al., 1988).

69 Due to the scarcity of seismic surveys and sediment coring, the Upper
70 Pleistocene-Holocene stratigraphy of the continental shelf off the southern RJ
71 margin remained poorly explored until Maia et al. (2010) recently addressed the
72 stratigraphic framework of the shallow sedimentary record (~300 ms) of this
73 area. The combined analysis of a recovered set of vintage sparker paper seismic
74 records (500-1000 J) acquired in the early 80's, chronostratigraphic data from
75 the **oil industry's exploratory wells** (Fig. 1) and $\delta^{18}\text{O}$ -derived information on
76 glaciation-related global sea-level variations (Marine Isotope Stages, MIS), led to
77 the identification of 5 major seismic sequences (Sq1-Sq5) interpreted as a
78 succession of depositional sequences induced by repeated glacioeustatic cycles of
79 alternating fall and rise, spanning the last ~500 kyr of the Quaternary. On the
80 interpreted sparker seismic lines, sequences Sq1-Sq4 enclose mainly outer shelf
81 progradational components (shelf wedge prisms) interpreted as relatively poorly-
82 preserved forced-regressive depositional sequences that each record a ~100-kyr
83 long glacioeustatic cycle, whereas the sedimentary unit labelled Sq5 was
84 interpreted to represent the transgressive and highstand deposition of the
85 current half-cycle (post-LGM, Holocene).

86 Thanks to the recent acquisition of a dataset of sub-bottom chirp profiles
87 (~500-5,500 Hz), that has been combined with existing bathymetric data, we
88 could for the first time look into the stratigraphic organization of shelf
89 sedimentary systems at a higher resolution, down to about 100 ms below the

90 seafloor. It was thus possible to explore the Upper Pleistocene-Holocene (last
91 ~120 kyr) shelf sedimentary architecture and recognize the aggradational and
92 highstand architectural elements contained within the uppermost seismic
93 sequences Sq4 and Sq5 identified by [Maia et al. \(2010\)](#). The datasets analyzed
94 allowed the reinterpretation of the stratigraphic meaning of the continuous
95 seabed features recognized across the continental shelf off southern RJ. In the
96 light of the present-day understanding of the high resolution seismic sequence
97 and Late Pleistocene to Holocene sea-level curves proposed worldwide, the origin
98 of the linear seafloor features are ascribed to distinct glacio-eustatic stages.

99 This research provides a case study of a relatively starved shelf from the
100 rather unexplored quaternary Brazilian continental margin, making unpublished
101 information available to a worldwide audience.

102

103 **2. BACKGROUND**

104 Landward of the **Santos basin's** northern sector lies the Serra do Mar, a
105 long coastal mountain range very close to the present day coastline. Tertiary
106 (Early Oligocene) tectonic reactivation events of this coastal mountain range led
107 to the reorganisation of drainage systems that delivered sediments directly into
108 Santos basin. Drainage systems were captured and diverted to the neighbouring
109 Campos basin and reorganised as the coast-parallel Paraíba do Sul river system
110 (Fig. 1) ([Modica and Brush, 2004](#)). As a consequence, the shelf environment
111 became relatively starved of clastic input. The shelf edge stepped back more
112 than 50 km landward of the Late Eocene position, to a position close to that
113 maintained at present. This configuration (Fig. 1) evolved into **today's** landscape
114 of narrow coastal plains and small rivers, draining mainly Precambrian crystalline
115 rocks, that terminate either directly into open sea or into the partially-enclosed
116 coastal environments such as Ilha Grande, Sepetiba and Guanabara bays

117 (Milliman, 1978; Zalán and Oliveira, 2005). The continental shelf off southern RJ
118 has thus been classically regarded as a sediment-starved shelf (e.g. Milliman,
119 1978; Kowsmann et al., 1977; Kowsmann et al., 1979; Kowsmann and Costa,
120 1979; Zembruski, 1979) developed in the context of a thermally-old and
121 tectonic stable margin (Chang et al., 1992; Caimnelli and Mohriak, 1999).

122

123 **2.1 Shelf morphology, oceanography and surface sediment distribution**

124 The study area is a low-gradient moderate- to high-energy continental
125 shelf, affected by the passage of winter frontal systems. It is a microtidal shelf
126 where tidal currents seem to be more important in the across-shelf direction
127 (Alves, 1992). The shelf break is irregular displaying large re-entrants and upper
128 slope morphological plateaus between Cabo Frio and São Sebastião island (Fig.
129 1), possibly related to the action of contour currents (Duarte and Viana, 2007).

130 The sudden change in margin orientation from E-W to NE-SW at Cabo Frio
131 Cape arguably is the most conspicuous geomorphic feature of the study area,
132 accompanied by important changes in shelf width and gradient. Off Cabo Frio
133 cape the 100-m isobath lies less than 10 km from the coastline, while farther
134 south it is located ~80 km away from Ilha Grande island (Fig. 1). The feature has
135 important implications for the shelf hydraulic regime and is associated with
136 changes in the Brazil Current (BC) trajectory (Signorini 1978; Campos et al.,
137 2000; Silveira et al., 2000; Rodrigues and Lorenzetti, 2001). The BC is a
138 western boundary contour current associated with the South Atlantic subtropical
139 gyre. It arises as a shallow and weak current at approximately 14.5–15.0° S
140 (Stramma and England 1999; Soutelino, 2008) becoming gradually deeper
141 (thicker) and stronger as it moves to the SW, roughly following the orientation of
142 the shelf break / upper slope. Between 22 and 23° S, the BC transports Tropical
143 Water (TW) and South Atlantic Central Water (SACW) in a depth zone bounded

144 by the water surface and the bottom of the pycnocline (Silveira et al., 2000).
145 Coastline configuration, continental margin bathymetry and the BC together
146 affect sedimentation patterns (Fig. 2) and geochemical characteristics of the
147 continental shelf and upper continental slope (Mahiques et al., 2004). Despite
148 the frequent occurrence of BC eddies around the Cabo Frio cape area (Silveira et
149 al., 2000; Mahiques et al., 2005; Calado et al., 2010), their influence on the
150 shelf and upper slope sediment dynamics remains largely unknown. Duarte and
151 Viana (2007) have discussed the role of BC eddies in reworking bottom sediment
152 and as an important erosive agent in the sculpturing of shelf-edge embayments
153 between Cabo Frio and São Sebastião island (Fig. 1). Recent studies by Nagai et
154 al. (2010), based on multiproxy analyses (sedimentology, geochemistry and
155 biostratigraphy), have highlighted changes in oceanic productivity and circulation
156 on the Brazilian southeastern upper continental margin for the last 27 kyr.
157 During the LGM, the fallen sea level, increased productivity and lowered sea-
158 surface temperatures may be considered the result of offshore displacement of
159 the main flow of the BC. During the post-LGM transgression, the increase in
160 water column temperature and more intense geomorphological work by the BC
161 suggest a displacement of its warm waters towards the coast.

162

163 **2.2 Quaternary stratigraphy**

164 Maia et al. (2010) first proposed a Pliocene-Quaternary stratigraphic
165 framework for the continental shelf off southern RJ, based on a combined
166 analysis of sparker seismic records (500-1000 J) acquired in the early 80's
167 (Geomar cruises; Fig. 3). The framework is composed mostly of stacked
168 clinoformal seismic units representing up to eight major seismic sequences
169 bounded by angular unconformities. According to their internal architecture and

170 the geometry of the recognized clinoforms, the seismic sequences were grouped
171 into two distinct stratigraphic sets identified as Set I (SqA-SqC) and Set II (Sq1-
172 Sq5). Reflectors S1 to S5 are erosive and frequently show stepped surfaces.
173 They truncate the underlying seismic sequences Sq1 to Sq4, as shown by many
174 toplap terminations. Surfaces S2, S3 and S4 bound sequences of limited updip
175 extent. The three surfaces merge landward with surface S1 to become shelf-wide
176 erosive surfaces. Each of these seismic horizons is interpreted as a master
177 sequence boundary, representing a diachronous period of erosion from during
178 times of deepest sea-level falls and lowstands, i.e. when subaerial exposure of
179 the shelf was most extensive. These surfaces (Fig. 3) were reworked during
180 subsequent times of sea-level rise.

181 Chronostratigraphic data (Nannofossil zonation) from oil-industry
182 exploratory wells enabled us to attribute an age younger than about 440-500 kyr
183 to the five seismic sequences of Set II (Maia et al. 2010; Fig. 3). Considering
184 that in their internal geometry and style of bounding surfaces, the sequences
185 Sq1-Sq4 mimic each other, it was proposed that they record fourth-order
186 depositional cycles of ~100-kyr periodicity, matching $\delta^{18}\text{O}$ -derived global sea-
187 level data (Fig. 3c). Sequence Sq5 does not reflect a depositional sequence in the
188 same sense as sequences Sq1-Sq4. Sq5 (of limited extent and thickness) would
189 represent transgressive and highstand deposition during the Holocene and be
190 part of a youngest sequence, just beginning its development (Fig. 3).

191 Due to the limited resolution of the sparker seismic reflection data,
192 depositional sequence Sq4 was poorly imaged in the mid-shelf while in the outer
193 shelf area only its progradational forced-regression components were clearly
194 identified. Sq5 was considered a rather unevenly distributed layer, interpreted
195 either to be an inner shelf highstand sedimentary prism, or to be patchy outer-
196 shelf transgressive sedimentary cover of local preservation favoured by erosive

197 depressions that would have pre-existed imprinted on surface S5. Surface S5
198 was thus mapped as representing the present-day seafloor across great parts of
199 the shelf (Fig. 3).

200

201 **3. MATERIAL AND METHODS**

202 The seismic stratigraphic and geomorphological analysis in this study
203 integrates 2D high-resolution seismic line data interpretations, newly acquired
204 high-resolution chirp seismic profiling and newly compiled bathymetric data (Fig.
205 1). The seismic dataset encompasses: (1) ~1,500 km of sub-bottom profiling
206 acquired in August 2010 during leg 2 of the oceanographic cruise RIO COSTA 1,
207 aboard the Brazilian *R/V Cruzeiro do Sul*. Acquisition was performed with a
208 surface tow Edgetech SB-501i sub-bottom profiler using full spectrum chirp
209 technology (signal frequency between ~500-5,500 Hz) that provides high-
210 resolution sub-bottom imagery of up to circa 100 ms penetration into the sub-
211 floor, with a vertical resolution of ~2-5 m; and (2) ~5,000 km of single-channel
212 vintage paper sparker seismic lines (500-1000 Joules, 100 to 1400 Hz), acquired
213 in the early 1980ies, during GEOMAR Oceanographic Cruises¹ (Fig. 1). Maximum
214 signal penetration ranged from 300 to 350 ms, while the vertical resolution
215 oscillated between 7 and 12 m, depending on the seismic line considered. To
216 calculate the thickness of each seismic sequence, an estimated layer velocity of
217 1600 m/s was considered. Analysis of seismic data followed established high-
218 resolution seismic and sequence stratigraphic methods (in terms of reflector
219 truncation and configuration), and allowed for identification of depositional

¹ A total of 24 legs of GEOMAR oceanographic cruises were carried out between 1972 and 1986 in a joint scientific programme between the Woods Hole Oceanographic Institute, Brazilian universities, governmental agencies and companies, aiming at the acquisition of seismic data, sub-bottom profiling and surficial-sediment sampling throughout the Brazilian continental shelf and slope.

220 sequences and their boundaries (Mitchum et al., 1977a; Mitchum et al., 1977b;
221 Catuneanu, 2006).

222 In the absence of swath bathymetric data, imagery of the sea-floor
223 morphology was achieved through the compilation of tens of Brazilian Navy
224 bathymetric sounding charts spanning over 50 years, made available by CHM-
225 Centro Hidrográfico da Marinha do Brasil (the hydrographic center of the
226 Brazilian Navy). This compilation of bathymetric data offered a horizontal
227 sampling of ~400m on the continental shelf (between water depths of ~20m and
228 ~200m) and ~1 km on the upper slope. For the continental slope, ETOPO2
229 regional data (Smith and Sandwell, 1997) was included, making up for the
230 relative low coverage of the navy's dataset.

231 As no deep cores are available on the shelf, we had no independent ages
232 of palaeoshorelines nor of measured or estimated sea-level curves established in
233 the area. In far-field tropical regions such as our study area, away from former
234 ice masses and related zones of marked glacio-isostatic effects, we could use as
235 a first approximation, a series of relatively precise global sea-level curves that
236 have been established based on analyses of deep sea foraminifera $\delta^{18}\text{O}$ isotope
237 records, calibrated by direct measurements of sea-level position extracted from
238 geological evidences (shoreline position) or using corals (e.g. Imbrie et al., 1984;
239 Chappel and Shackleton, 1986; Labeyrie et al., 1987; Fairbanks, 1989; Bard et
240 al., 1990; Bassinot et al., 1994; Szabo et al., 1994; Lambeck, 1997; Rohling et
241 al., 1998; Toscano and Lundberg, 1999; Shackleton, 2000; Lambeck and
242 Chappell, 2001; Waelbroeck et al., 2002; Cutler et al., 2003; Rabineau et al.,
243 2006); or still using stratigraphic models (e.g. Skene et al., 1998) and a
244 hydraulic model of water exchange (Siddal et al., 2003), as synthesized in
245 Rabineau et al. (2006).

246

247 **4. RESULTS**

248

249 **4.1 Shelf seafloor morphology**

250 The E-W-oriented continental shelf of the study area extends for about 400
251 km from Cabo Frio cape, on the east, to São Sebastião island, on its western
252 limit (Figs. 1 and 4). This shelf has a gentle mean gradient of $\sim 0.04^\circ$ and
253 becomes steeper offshore Sepetiba-Ilha Grande bays ($\sim 0.07^\circ$, Fig. 4f-h), where
254 the shelf width reaches circa 125 km (Fig. 4f). In fact, the definition of shelf
255 width and shelf break depth is not always easy to apply in this area, since shelf-
256 edge and upper slope morphologies are irregular due to the occurrence of strong
257 erosional and/or gravitational collapse features (see below). Using the classical
258 methods for determining the shelf break position and depth (e.g. [Stanley and](#)
259 [Moore, 1983](#)), we found that it increases from -160 m in the east, off Cabo Frio
260 (Fig. 4a), to -177 m in the west, off Ilha Grande bay (Fig. 4f). Off São Sebastião
261 island, the shelf break at -148 m is shallower again (Fig. 4h).

262 Two main NW-SE-oriented elongated depressions were mapped along the
263 mid-outer continental shelf: the Eastern and the Western Corridors (Fig. 5). We
264 define the mid-outer shelf as the portion of the continental shelf seaward of the
265 100-m isobath. The Western Corridor corresponds to a zone of deeper erosion
266 (~ 30 m), in comparison to the Eastern Corridor which shows a shallower erosion
267 (~ 15 m; Figs. 4 and 5). A composite bathymetric and gradient map, drawn on
268 the basis of the newly compiled bathymetric data, highlights the main
269 geomorphic features that constitute the shelf seafloor morphology as well as
270 their spatial variability (Fig. 6). At the regional scale, the 100-m isobath marks a
271 clear transition between two contrasted landward and seaward shelf
272 morphologies.

273 Landward of the 100-m isobath, the sea-floor shows a remarkable lobate
274 and smooth morphology, whose front slope dips about 0.2° , along a ~ 8 -10 km
275 wide zone bracketing the 100-m isobath, forming a prominent sea-floor step
276 (Figs. 4, 6 and 7). In map view, this wide zone forms a linear and continuous NE-
277 SW-oriented bedform feature that draws away from the coastline westwards
278 (Figs. 5 and 6), and exhibits distinct shapes in east-west orientation. Offshore of
279 the Cabo Frio-Araruama lagoon region, the inner to mid shelf domain is defined
280 by a continuous, slightly concave-up and rather steep sea-floor ramp ($\sim 0.255^\circ$;
281 Fig. 4b) whereas westwards, a convex-up profile draws a clear lobate shape on
282 the sea-floor (Figs. 4c-d and 7). A succession of nine major lobate seabed
283 features is also observed landward of the 100-m isobaths (numbered 1 to 9 in
284 Fig. 5). The features are elongated or semi-circular sediment bodies expressed
285 by increased sea-floor gradient roughly coinciding with the 20/30, 40/50m and
286 60/70-m isobaths. The most distinguishable of these bathymetric steps are
287 located on the western shelf, off Ilha Grande, Sepetiba and Guanabara bays
288 (Figs. 4 and 5).

289 Seaward of the 100-m isobath, the shelf gradient decreases to about
290 0.023° - 0.051° (Figs. 4 and 6), and the seafloor is covered by an array of
291 contour-parallel escarpments. These linear features form at least three
292 escarpments of regional expression, roughly NE-SW-oriented, that run along the
293 ~ 110 , ~ 130 and ~ 150 -m isobaths. All the escarpments stand as fairly
294 continuous contour line features when considering the ~ 400 km lateral extent of
295 the shelf. Nonetheless, they exhibit distinct relief, continuity and contour shapes
296 in map view (Figs. 5 and 6):

297 -Scarps at ~ 110 m are ~ 5 -8 m high, exhibit an average 0.2° gradient, and are
298 followed by wide and flat basal surfaces, as wide as 20 km (Figs. 6, 7 and 8a).

299 The linear escarpment tends to merge westwards with the ~8-10 km wide
300 zone bracketing the 100-m isobath, forming one unique prominent sea-floor
301 step (Fig. 5);

302 -Scarps at -130 m are ~10-20m high, exhibit up to 0.4° gradient, and are
303 followed by a basal surface, ~5-15 km wide (Figs. 6, 7 and 8). This
304 escarpment draws the most sinuous trace on the modern bathymetry, showing
305 some quite sinuous re-entrants, and disappears along segments of the
306 Western shelf Corridor (Fig. 5);

307 -The distal -150 m escarpment follows a straighter feature closely to the
308 bathymetric contour line, but occurs only along the main shelf-edge
309 embayments (Fig. 5). This escarpment presents quite variable relative relief,
310 ranging from a few meters to almost 60 m, either being prolonged seaward
311 by a basal flat surface, as wide as ~5 km, or grading into a larger seaward-
312 inclined erosive ramp presenting significant slopes of up to ~0.75° (Figs. 6
313 and 9). Along a few sectors of the two shelf-edge embayments, the
314 escarpment is coupled with a highly erosive and deep basal channel incision
315 tens of kilometers long, ~8-10 km wide and ~40-50 m deep, described for the
316 first time in this study (Figs. 4 and 9c).

317

318 **4.2 Seismic and chronostratigraphic interpretation**

319 So far, in this paper we adopted a chronostratigraphy as had been
320 established by Maia et al. (2010). However, the newly obtained high-resolution
321 chirp seismic profiles revealed that shallow sequences Sq4 and Sq5 are
322 stratigraphically more complex and exhibit a more distinctly lateral distribution
323 than had been previously recognized. Moreover, the combination of bathymetric

324 data and seismic profiling illustrates the various morphologies and stacking
325 patterns related to the Latest Quaternary history of the shelf sedimentary
326 system.

327

328 **4.2.1 Refined stratigraphic architecture of sequence Sq4**

329 On the inner to middle shelf, sequence Sq4 can build up lobate
330 depositional units, with an estimated thickness of circa 20-25 m. As a general
331 pattern, this wedge is composed of the stacking of at least two seismically
332 transparent units (sub-units Sq4a and Sq4b; Fig. 7). Reflections at the distal end
333 of these units show clinofolds, suggesting progradation (e.g. [Mitchum et al.,](#)
334 [1977b](#)). Erosive surfaces constitute the top limits of the upper and lower seismic
335 sub-units Sq4a and Sq4b (surfaces S5 and S5', respectively) depicting incisions
336 that on average are up to 10 m deep and ~50 m wide, with local evidence of
337 developed incised valleys (Fig. 7). According to its position along the depositional
338 profile, seismic facies and overall backstepping stacking pattern, we interpret this
339 proximal wedge as representing vertical sediment accumulation formed during
340 transgression (transparent facies), interrupted by a sea-level drop and partial
341 lowstand shelf exposure (unconformities S5' and S5 followed by distal
342 clinofolds).

343 Given the tectonic stability of the RJ margin over the Late Pleistocene-
344 Holocene period and its tropical location away from glaciations (e.g. [Chang et al.,](#)
345 [1992](#); [Cainelli and Mohriak, 1999](#)), we used global eustatic sea-level curves
346 (Fig. 10) in order to bring some paleobathymetrical-chronological constraints to
347 our uppermost stratigraphic units. The interpretation of seismic sub-units Sq4a
348 and Sq4b in the light of independent sea-level curves suggest them to result
349 from oscillations in the course of the Late Pleistocene sea-level fall. The

350 elevations of sub-units Sq4a and Sq4b along the depositional profile make us
351 interpret them to have formed during Marine Isotope Substages 5e-5a and MIS
352 4, when sea level fell from a few meters above to circa 100 m below present sea
353 level, with considerable intermediate oscillations (Figs. 7 and 10a). As such, this
354 proximal composite sedimentary wedge, in spite of representing gradual Late
355 Pleistocene sea-level lowering, may be interpreted as a late Highstand Systems
356 Tract (IHST; [Catuneanu, 2006](#)), that is topped by a surface formed by forced-
357 regression. Seawards, this composite lobate wedge grades into higher angle
358 parallel-oblique prograding clinoforms, reflecting the offlapping forced-regressive
359 wedges that extend as far as the distal end of the shelf break. These offlapping
360 wedges are the dominant stratigraphic elements of a Falling-Stage Systems Tract
361 (FSST; [Plint and Nummedal, 2000](#)), presumably formed during MIS 3 and MIS 2
362 (Figs. 7 and 10).

363 The new dataset also shows that the earlier interpretation of Sq4 as a
364 continuous sequence across the entire mid-outer shelf was too simplistic. Sq4 is
365 somewhat eroded in the Eastern Corridor, and deeply or totally eroded in the
366 Western Corridor, where neither a proximal Sq4 HST, nor distal FSST deposition
367 is well preserved. On the other hand, evidence for associated incised valleys is
368 widespread (Figs. 11 and 12). In addition, seismic profiles also revealed a spatial
369 relationship between the shelf corridors as zones of enhanced erosion, and the
370 sinuosity and lateral continuity of the -110 m and -130 m escarpments. Within
371 the Eastern Corridor, the -110 m and -130 m escarpments tend to present a
372 more sinuous trace, whereas within the Western Corridor these both
373 escarpments are missing (Figs. 5 and 12). We associate the enhanced erosion in
374 the shelf corridors with increased fluvial incision, that gradually propagated
375 upstream from the shoreline in order to balance the increasing base-level
376 lowering, thus leading to the escarpments' trace retreat. In the Western Corridor,

377 Sq4 has been so deeply eroded that S5 merges with S4 into a single, flatter
378 unconformity erosional surface (Figs. 11 and 12). Enhanced erosion within the
379 Western Corridor is also seismically indicated by a cyclical pattern of fluvial
380 incision-infilling that repeats through time on both surfaces S5 and S4, as
381 widespread features extending from the inner to the outer shelf (Fig. 12).
382 Increased erosion within this shelf corridor can explain the local removal of
383 sequence Sq4, the flattening morphology of the merging surfaces S4-S5 as well
384 as the absence of the -110 m and -130 m escarpments (Figs. 11 and 12).

385

386 **4.2.2 Refined stratigraphic architecture of the uppermost sequence Sq5**

387 We here present a revised architectural interpretation of sequence Sq5 of
388 [Maia et al. \(2010\)](#). The high-resolution chirp seismic lines show that this
389 youngest sedimentary unit covers the entire shelf landward of the 150 m deep
390 escarpment as a tabular unit, whereas towards the shelf edge, the seabed
391 consists exclusively of older S4 regressive wedges (Figs. 7 and 12). This means
392 that the basal surface S5 does not represent the modern seafloor along its entire
393 extent, unlike previously proposed (Fig. 3), but rather is a somewhat older
394 erosional horizon with several steps and seaward dip: S5 represents the last
395 lowstand exposure surface. It is overlain by the Sq5 deposits, observed
396 widespread throughout the shelf (Fig. 7). The stratigraphic position of this top
397 sedimentary unit supports the interpretation of it as being the product of latest
398 Pleistocene-Holocene gradual deposition that began when the last deglaciation
399 began, i.e. not solely as Holocene deposition.

400 The seismic data do not show clear internal patterns within the tabular Sq5
401 sedimentary units across the mid-outer shelf. Instead, the unit appears
402 acoustically transparent, and was thus interpreted as a transgressive siliciclastic

403 sheet (Figs. 8, 11 and 12). Its thickness is however highly variable across the
404 shelf. Relative thicker deposition (up to ~15 m) is observed throughout the
405 western shelf sector, encompassing the Western Corridor and the adjacent shelf,
406 where it fills depressions in the underlying S5 erosional surface (Fig. 11).
407 Widespread fluvial incision-infilling patterns, seismically recognized on the
408 western shelf sector in Sq4 and the thicker Sq5, indicate relatively higher
409 sediment supply to this sector after the LGM (Fig. 12).

410 On the inner shelf, Sq5 sedimentation to some degree has piled up as
411 prism-like depositional features, maximizing at 8-10 m thickness only locally
412 (Fig. 5). In the central shelf sector, this sedimentary unit is composed of frontal
413 progradational foresets with no clear seismic evidence of significant erosion (Fig.
414 13b). Sparse coverage and limited resolution of seismic data makes it difficult to
415 further detail the internal architecture of these features. Nevertheless, the most
416 distinguishable of these prism-like features are located off Guanabara bay where
417 they form major semi-circular bathymetric steps, that roughly coincide with the
418 ~20, ~30 and ~40-m isobaths (numbered 1 to 3 in Fig. 5). In the western shelf
419 sector, the prisms pile up as backstepping transparent depositional units with
420 smaller-scale rough morphology; a few of them have smooth bathymetric bulges
421 at their distal ends (Figs. 13c). This generates elongated and laterally-
422 discontinuous higher-gradient steps on the sea-floor slope, that locally coincide
423 with the ~50, ~60 and ~70-m isobaths (numbered 4 to 9 in Fig. 5).

424 The entire seafloor morphology seaward of the 100-m isobath is also
425 affected by relatively high frequency rugged relief superimposed on the scarp-
426 terraces previously described (Figs. 7, 9, 11 and 12). This micro relief is ascribed
427 to the occurrence of the bioconstructional forms, as have been previously
428 reported for the study area (Milliman, 1978; Figueiredo and Tessler, 2004). On
429 higher-resolution seismic lines these features appear to be up to ~10 m thick,

430 and relative large areas of the sea-floor are covered with these carbonate build-
431 ups. In places they clearly overly clastic transgressive Sq5 facies (Fig. 14), which
432 makes these bioconstructions part of the Sq5 HST.

433

434 **5. DISCUSSION**

435 From various siliciclastic continental shelf settings around the world,
436 studies provide examples of seafloor geomorphologies affected by the last
437 transgression, with the youngest transgressional features identified as purely
438 depositional, or purely erosional or a composite of both (e. g. [Emery and Uchupi,](#)
439 [1984](#); [Milliman et al., 1990](#); [Correa, 1996](#); [Duncan et al., 2000](#); [Lobo et al.,](#)
440 [2004](#); [Bassetti et al., 2006](#); [Berné et al., 2007](#); [Schattner et al., 2010](#)). In such
441 studies, typically based primarily on high-resolution seismic stratigraphy and
442 occasional drill holes, linear stepped shelf bathymetric features are often tied to
443 periods of decelerated sea-level rise or stillstands during the last transgression.
444 Those shelves are either sediment-starved, such as the New Jersey shelf (e.g.
445 [Duncan et al., 2000](#)), or are under high sediment input, such as the submerged
446 Rhône deltaic system (e.g. [Berné et al., 2007](#)). A recent review and synthesis of
447 transgressive deposit types is presented by [Cattaneo and Steel \(2003\)](#).

448 Despite the current controversy over the exact sea-level position at the
449 LGM (a fall as modest as -90 m or as deep as -140 m), global sea-level data
450 based on independent proxies and modelled reconstruction, from the end of the
451 LGM onwards indicate global sea levels to have risen dramatically: fast and by a
452 great amount, but non-uniformly (e.g. [Fairbanks, 1989](#); [Bard et al., 1990](#); [Bard](#)
453 [et al., 1996](#); [Lambeck and Bard, 2000](#); [Lambeck et al., 2002](#); [Lambeck et al.,](#)
454 [2004](#); [Clark, 2009](#); [Berné et al., 2007](#); [Bard et al., 2010](#)). The first order rate of
455 sea-level rise averaged over the entire deglaciation (~20 ka to present) is
456 around 5-6 m/kyr. But this deglaciation is known to have been characterized by

457 two or three periods of increased rates of rise, including so-called Melt Water
458 Pulses, separating periods of much lower rates (Fairbanks, 1989; Bard et al.,
459 1990). The sea level for the latter periods would be indicated by elevation steps
460 at sea levels ~100, ~60 and ~40 m below present, the last one overstepped by
461 sea-level rise acceleration at the beginning of the Holocene (Fig. 10b).

462 However, in our combined seismic and geomorphological interpretation,
463 transgressive morphological features from the shorter period of sea-level rise in
464 the last ~20 ka are very scarce and limited to the present inner-shelf, where
465 they appear as laterally-discontinuous depositional prisms forming local
466 bathymetric steps. Our seismic analysis and timing deductions indicate that the
467 linear, stepped bathymetric features have the same spatially relation across the
468 entire shelf and link to a set of architectural elements that developed over the
469 much longer lasting phase of Late Pleistocene sea-level lowering, regression and
470 shelf exposure towards the LGM, i.e. between ~120 and ~20 ka (Fig. 15). On the
471 outer shelf, transgressive and highstand deposits are limited to a thin veneer of
472 reworked material and coral carbonate bioconstructions with a distinct
473 transparent chirp facies (Figs. 7 and 11).

474

475 **5.1 Geomorphic indicators attributable to stratigraphic elements and dynamic** 476 **processes of the Late Pleistocene regression (~120 to ~20 ka)**

477 In spite of the blanketing presence of Sq5 deposition, a prominent
478 regional-scale sea-floor step that brackets the 70-100 m isobaths stand out in
479 the modern bathymetry (Figs. 5 and 6). It is the morphological expression of the
480 spatial discontinuity and stratigraphic gap between the proximal and the distal
481 stratigraphic elements of last completed sequence Sq4, formed over the ~100
482 kyr of the Late Pleistocene. From this sequence Sq4, a partially preserved HST
483 remains proximal on the shelf, and a distal FSST remains down-dip (section
484 4.2.1; Fig. 7). As shown in a conceptual stratigraphic model proposed in Figure

485 16, we related this stratigraphic gap to the eustatic sea-level regressive scenario
486 between MIS 5e and MIS 2 (Late Pleistocene): (A) At **t0** (MIS 5d) the
487 depositional profile of shelf sediments consists of forced-regressive Sq3 wedges,
488 previously deposited during stages of falling sea level between MIS 7 and MIS 6,
489 while the shoreline is on the middle shelf off southern Rio de Janeiro State. Sea
490 level rises rapidly between **t0** and **t1** (MIS 5c) resulting in the deposition of
491 transgressive prisms on the inner shelf; (B) sea level drops between MIS 5c and
492 MIS 5b (**t2**) and induces erosion on the shelf that partially reworks the previously
493 deposited transgressive prism, while further on the outer shelf a new prism
494 forms. The final sedimentary motif is a composite transgressive-prograding
495 clinoform preserved as sub-unit Sq4a. Unconformity S5' thus reflects the shelf's
496 partial exposure at **t2**; (C) sea level then rises rapidly again between **t2** and **t3**
497 (MIS 5a) and then (D) drops towards **t4** (MIS 4), inducing vertical accumulation
498 of a second composite transgressive-regressive wedge (subunit Sq4b). The
499 ensuing regressive sea-level trend between **t4** and **t6** (E and F) partially erases
500 the previous sediment accumulation, leading to the deposition of offlapping
501 forced-regressive Sq4 wedges that extend as far as the distal end of the shelf
502 break (a FSST). We interpret this erosional gap and the observed change of dip
503 in surface S5, as indicating the outpacing of the relatively low rate of sediment
504 influx (which characterizes this shelf; [Milliman, 1978](#); [Rocha et al., 1975](#)), by the
505 ongoing sea-level fall and the steadily accelerating base-level lowering from
506 MIS 3 to MIS 2 (Fig. 10a). An outpaced sediment flux can explain, at least in
507 part, the stratigraphic discontinuity between highstand and regressive deposits in
508 the down-dip direction. Nonetheless, Sq4 forced-regressive wedges did preserve
509 on the outer shelf, showing that the sediment flux was sufficient to fill some
510 accommodation space on the shelf, i.e. that progradation kept up with rates of
511 sea-level fall (Figs. 3 and 7).

512 For the study area, no estimates of sediment influx are available, nor core
513 data from which sedimentation and sea-level variation could be reconstructed,
514 not for the Late Pleistocene and not for the post-LGM. Still, based on the
515 envelope of the compiled global sea-level data (the maximum variability interval;
516 Fig. 10a), we reckon that the partial preservation of the HST of sequence Sq4 is
517 due to the fact that MIS 5e was represented by a relatively high sea-level
518 position (meters above current sea level) compared to highstands before and
519 after (Fig. 10a), whereas the lowstand in the LGM is generally considered to have
520 been at a shallower level, and lasted less long, than the penultimate lowstand
521 (the MIS 6 glacial maximum; Fig. 10a). Such offset between subsequent cycles
522 can possibly explain why part of Sq4 represents late HST deposits (Fig. 8).

523 Throughout the study area, the appearance of the Sq4 proximal wedge
524 varies considerably in the across shelf direction, probably due to variable
525 sediment supply. In the eastern shelf domain, its thickness does not exceed ~8
526 m and prograding units are absent, resulting in a continuous and slightly
527 concave-up sea-floor profile. Therefore, this depositional wedge, although
528 marking a transition in the sea-floor slope around the 100-m isobath, does not
529 seem to have impacted the modern sea-floor morphology across this shelf sector
530 (Fig. 13a). On the central-western shelf, where substantially larger sediment
531 supply reached areas off the Guanabara, Sepetiba and Ilha Grande bays, sets of
532 internal acoustic facies are quite distinct: composed of thicker transparent series
533 with developed prograding foresets and deeply incised valleys (Fig. 13b). This
534 composite prograding wedge generated a prominent convex-up seafloor
535 bathymetry forming the step-like bedform that appears as a continuous
536 morphological feature along the 100-m isobath, extending over 250 km in an E-
537 W direction in the central and western shelf domains of the study area (Fig. 15).

538 Another outstanding morphological signature of sequence Sq4 is the
539 offlapping seaward-downstepping character of its distal stratigraphic elements,
540 forming detached forced-regressive wedges that became gradually deeper and
541 younger spreading over 40-60 km towards the shelf break (section 4.2.1; Figs. 7
542 and 8). The combined seismic and morphological analyses allowed to spatially
543 associate the fairly continuous -110 m linear escarpment and its coupled
544 seaward-dipping terrace, to an erosional remnant of offlapping shorelines still
545 preserved in the modern shelf morphology. Accordingly, we associated its
546 ~5-10 m relief with a sort of footprint of detached downstepping wedges formed
547 during the Late Pleistocene sea-level fall, with little reworking and marine
548 obliteration during the subsequent rapid transgression. Considering the seismic
549 resolution of the available dataset, the -110 m escarpment appears then as a
550 purely erosional inclined feature on the modern bathymetry, while the associated
551 basal seaward-stepping terrace sculpted on surface S5 is all over capped by a
552 transgressive Sq5 sediment layer (Figs. 7 and 15).

553 In the light of the available eustatic sea-level curves, we speculate that
554 such downstepping forced-regressive morphology observed on the mid-outer
555 shelf probably formed at *t5*, the inflection point of the regressive curve,
556 explained by accelerating sea-level fall during MIS 3 and into MIS 2 (Fig. 16 E
557 and F). In fact, it is worth noting that similar erosional remnants imprint seaward
558 subaerial exposure surfaces S4 and S3 (respectively, top and basal boundary of
559 sequence Sq3) and also draw steps of the order of a few meters high towards
560 their respective palaeo-shelf breaks. This cyclical pattern of seaward
561 downstepping terraces actually shows that they are recurrent geomorphic
562 features developed during ~100 kyr long lasting periods of successive sea-level
563 lowstands and shelf exposure of the continental shelf of the study area (Fig. 3).

564

565 **5.2 Geomorphic indicators attributable to stratigraphic elements and dynamic**
566 **processes at the LGM (~20 kyr)**

567 As shown in section 4, the most distinguishable continuous relief feature
568 mapped across the continental shelf off southern RJ is the modern bathymetric
569 footprint of the boundary surface S5 (Figs. 7 and 8), that in earlier studies had
570 been interpreted as a prominent shelf-wide unconformity (Maia et al., 2010).
571 High resolution seismic reflection profiles interpreted for this study also showed
572 that S5 truncates the underlying units but with distinct patterns of erosion.
573 Landward of the 130-m isobath, S5 is a smooth downstepping and seaward
574 dipping surface capped by younger Sq5 seismic strata. Seaward of the 130-m
575 isobath, S5 shows more pronounced erosion and limited Sq5 cover (Figs. 7 and
576 8). In spite of the total absence of direct measurements and datings in the study
577 area, we suggest that the linear scarp mapped around the -130 m contour line is
578 the regional geomorphic indicator of the LGM sea-level position (At **t6** in Fig. 16
579 F). Wave-cut erosion must be evoked for the generation of such an outstanding
580 morphological feature, compatible with prolonged wave action during a stillstand
581 (Fig. 8). As a consequence, we no longer interpret S5 as an exposure surface
582 across its whole extent. Landward of the 130-m isobath S5 would have been a
583 subaerial surface whereas seaward of this depth it would have been a purely
584 marine surface (Figs. 8 and 15). Finally, we note that the Sq5 transgressive layer
585 and carbonate bioconstructions can add up to 10 m to the scarp's total relative
586 relief thus enhancing the scarp (Figs. 8 and 14).

587

588 **5.3 Geomorphic indicators attributable to stratigraphic elements and dynamic**
589 **processes of the post-LGM transgression (last ~20 kyr)**

590 The -150 m escarpment expresses itself as a morphological feature linked
591 to the youngest distal shelf clinoform, at around 20-30 m below the basal terrace
592 of the -130 m escarpment (Fig. 8b). Seismic data show a large shelf edge zone

593 affected by intense bottom erosion with exposure of relict strata seaward of the
594 150-m isobath down to the offshore limit of the available seismic imagery,
595 beyond the 250-m depth contour (Figs. 7, 8, 9 and 12). In contrast with the
596 -130 m scarp, this deeper escarpment in the distal zone of major shelf-edge
597 erosion is attributed to marine erosion that is unrelated to wave action. We
598 interpret its formation to be associated with landward displacement and
599 enhanced bottom erosion of the southward flowing BC, during the last
600 transgression (Figs. 8 and 16 F). This would be in accordance with studies
601 carried out by [Nagai et al. \(2010\)](#), that integrated sedimentological, geochemical
602 and microfaunal proxies, as well as with a conceptual model proposed by
603 [Mahiques et al. \(2007\)](#). This means that the -150-m escarpment along the two
604 large shelf-edge embayments described in section 4.1 (Figs. 9 and 15), as well
605 as its associated basal channels, are seen as post-LGM features. Previous studies
606 have proposed that exposure of relict Pleistocene facies at shallower bathymetric
607 levels equivalent to the mid-shelf (i.e. the ~130-m isobath) was due to a "floor-
608 polisher" effect of the meandering BC main flow ([Mahiques et al., 2002](#);
609 [Mahiques et al., 2010](#)). Although we do consider such a sculpturing role for the
610 shelf edge, our architectural seismic analysis revealed the presence of a
611 continuous tabular Sq5 transgressive layer throughout the entire mid-outer shelf,
612 implying that it was not significant on the mid-shelf.

613 Laterally-discontinuous stepped bedforms located on the inner shelf
614 landward of the 100-m isobath are also interpreted as geomorphic indicators of
615 stratigraphic elements of the post-LGM transgression. However, while previous
616 studies describe inner-shelf stepped features as probably representing stillstand
617 shores ([Zembruski, 1979](#); [Corrêa et al., 1980](#)) and thus as being, at least
618 partially, erosional in nature, the new seismic evidence shows that, on the
619 contrary, they may be fully depositional features. In the central shelf sector, off

620 Guanabara Bay, the mapped bedforms are essentially depositional Sq5 prism-like
621 sediment bodies, exhibiting external lobate shapes that suggest progradational
622 bedforms that roughly coincide with the 20, 30 and 40-m isobaths (Figs. 5, 13
623 and 15). Limited seismic resolution and the absence of direct sampling and
624 dating make it impossible to explain the construction of these features or to
625 establish their exact eustatic position during the post-LGM transgression. They
626 may represent the preservation of shorelines and shorefaces that had developed
627 during periods of relatively slower sea-level rise in the Early Holocene, around
628 the present-day 30-40m isobath (Fig. 9b). We can equally speculate that they
629 correspond to subaqueous deposition on the inner-shelf during highstand
630 scenarios thus representing infra-littoral prisms (*sensu* [Hernandez-Molina et al,](#)
631 [2000](#); [Fernández-Salas et al., 2009](#)) as, for instance, the modern features
632 developed at the mouth of Guanabara Bay (probably under the influence of
633 strong tidal currents). In the western shelf sector, on the other hand, Sq5 is
634 mostly composed of transparent seismic units stacked in backstepping fashion,
635 and this strongly suggests it to reflect transgressive deposition. On the available
636 seismic lines, these units pinch-out seaward around the 60 and 70-m isobaths,
637 without major morphological expression on the modern bathymetry (Fig. 5, 13c
638 and 15).

639

640 **5.4 Pleistocene sediment supply to the shelf**

641 This seismic stratigraphic framework points thus to an effective sediment
642 supply to the shelf basin during most of the time in the Late Pleistocene, a
643 scenario that contrasts with the current idea of dominantly sediment-starved
644 Late Pleistocene shelves. Our results naturally raise questions about the nature
645 and origin of the sediment supply, since nowadays no significant siliciclastic

646 fluvial point source flows directly into the shelf. We are led to speculate about a
647 more important participation of secondary drainage basins that presently
648 debouch directly into partially-enclosed coastal environments, like the Guanabara
649 and Sepetiba bays, to have supplied sediment to the adjacent shelf (as recently
650 pointed out by Friederichs et al.; in press); we may also have to consider the
651 possible role of neotectonic movements involving the Serra do Mar coastal
652 mountain ranges that, at times, might have been the source of the clastic influx
653 into the basin during the Quaternary.

654

655 **CONCLUSIONS**

656

657 Our paper addresses the bathymetric and seismic mapping of Upper
658 Pleistocene submerged geomorphological elements and the origin of encountered
659 linear, stepped features observed along the continental shelf off southern Rio de
660 Janeiro state, northern Santos basin. Newly obtained high resolution seismic
661 reflection records (down to about 100 ms penetration below sea-floor), revealed
662 the higher-resolution stratigraphic organization of shelf sedimentary systems,
663 telling the **shelf's** history since MIS 5. Even in the absence of independent
664 biostratigraphical or numerical ages, the analysis allows to identify features
665 associated to youngest sea-level falls from those formed during youngest sea-
666 level rise. Because the study area is a far-field tropical shelf, global eustatic sea-
667 level curves then provide chronological constraints for transgressive and
668 regressive features in known order at known depths.

669 Unit Sq4 is the depositional sequence representing ~120 to 20 ka. On the
670 inner shelf, it comprises of proximal lobate depositional units (as thick as ~20-25
671 m), that grade into prograding clinoforms, extending as far as the distal end of

672 the shelf break as offlapping forced-regressive wedges with vertical sediment
673 accumulation as thick as ~40-50 m. This sequence stopped accumulated when
674 the shelf was exposed during the lowstand of the LGM (ca. 25-20 ka). Following
675 the LGM, transgressive sedimentation (Unit Sq5, up to ~15 m thick) has
676 blanketed the continental shelf landward of an escarpment at 150 m depth.

677 Regarding the shelf morphology, most of the linear stepped features found
678 across the continental shelf off southern Rio de Janeiro State are actually of Late
679 Pleistocene age, formed under regressive conditions, with some sediment supply.
680 Present-day conspicuous bathymetric steps mapped at -110, -130 and -150m
681 have diverse geomorphic features and were related to the sea-level variations
682 spanning the last interglacial-glacial-interglacial cycle. The -110 m escarpment is
683 an erosional imprint of offlapping stepped forced-regressive wedges that were
684 probably sculpted between MIS 3 and MIS 2. The -130 m escarpment relates to
685 the shoreline position during the LGM. As for the -150 m scarp, we suggest this
686 to be formed in response to shelfward migration of the Brazil Current,
687 accompanying the sea-level rise during the last transgression. Transgressive and
688 highstand morphological imprints of the rapid sea-level rise of the post-LGM
689 (youngest ~20 kyr) are extremely scarce and limited to the current inner-shelf
690 only, where they appear as laterally-discontinuous depositional prisms forming
691 local bathymetric steps offshore Guanabara, Sepetiba and Ilha Grande bays,
692 through which a substantially large sediment supply reached the drowning shelf.

693

694 **ACKNOWLEDGEMENTS**

695 This research was funded by a program of concerted action between the
696 Brazilian Ministry of Science, Technology and Innovation (MCTI) and the
697 Brazilian Navy for the advancement of scientific oceanographic investigation

698 through the availability of ship time. The study was also partially funded by
699 CAPES (Coordination for the Improvement of Higher Level Education, "*Ciências*
700 *do Mar*", grant 23038.051609/2009-61), FAPERJ-Research Agency of Rio de
701 Janeiro State (grants 110.812/2008, 111.516/2008, 110.161/2009,
702 101.519/2009 and 102.254/2009) and CNPq-the Brazilian National Research
703 Agency (*Universal grant 474004/2010-4*). This work further benefited from a
704 State Grant from the French "Agence Nationale de la Recherche (ANR)" in the
705 Program "Investissements d'Avenir" (ANR-10-LABX-19-01, Labex Mer), and
706 international research grants by Institut Universitaire des Sciences de la Mer
707 (IUEM) and Université de Bretagne Occidentale (UBO), France.

708 The authors gratefully acknowledge the contribution of the captain and
709 crew of *R/V Cruzeiro do Sul* in the acquisition of seismic data during leg 2 of RIO
710 COSTA 1 Cruise (August 2010). We thank the CHM-Centro Hidrográfico da
711 Marinha do Brasil for sharing their bathymetric database. Special thanks are due
712 to Seismic Micro-Technology Inc. (SMT) for the use of educational licenses of the
713 software Kingdom Suite® and CNPq for the research grants conceded to the first
714 and third authors, and scholarships to undergraduate students (PIBIC/CNPq). We
715 are grateful to two anonymous reviewers for significantly improving the work
716 with their insightful comments. We also thank the Editor Kim Cohen for
717 constructive suggestions and constant support to this paper. This is a
718 contribution of the research group GEOMARGEM-Geology and Oceanography of
719 Passive Continental Margins (<http://www.geomargem.org>).

720

721 **REFERENCES**

722

723 Alves, M.A., 1992, Correntes de maré e inerciais na plataforma continental ao
724 largo de Ubatuba (SP). Master Dissertation, Instituto Oceanográfico da
725 Universidade de São Paulo (USP), 162 pp. São Paulo, Brazil (in Portuguese).

726 Bard, E., Hamelin, B., Fairbanks, R.G., 1990. U-Th ages obtained by mass
727 spectrometry in corals from Barbados: sea level during the past 130,000
728 years. *Nature* 346, 456–458.

729 Bard, E., Hamelin, B., Arnold, M., Montaggioni, L., Cabioch, G., Faure, G.,
730 Rougerie, F., 1996. Deglacial sea-level record from Tahiti corals and the
731 timing of global meltwater discharge. *Nature* 382, 241–244.

732 Bard, E., Hamelin, B., Delanghe-Sabatier, D., 2010. Deglacial Meltwater Pulse 1B
733 and Younger Dryas Sea Levels Revisited with Boreholes at Tahiti. *Science*
734 327, 1235-1237.

735 Bassetti, M.A., Jouet, G., Dufois, F., Berne, S., Rabineau, M., Taviani, M., 2006.
736 Sand bodies at the shelf edge in the Gulf of Lions (western Mediterranean):
737 deglacial history and modern processes. *Marine Geology*, 234, 93–109.

738 Bassinot, F., Labeyrie, L., Vincent, E., Quidelleur, X., Lancelot, N.J., Lancelot,
739 Y., 1994. The astronomical theory of climate and the age of the Brunhes-
740 Matuyama magnetic reversal. *Earth and Planetary Sciences Letters* 126, 91–
741 108.

742 Berné, S., Jouet, G., Bassetti, M.A., Dennielou, B., Taviani, M., 2007. Late Glacial
743 to Preboreal sea-level rise recorded by the Rhône deltaic system (NW
744 Mediterranean). *Marine Geology* 245, 65–88.

745 Cainelli, C., Mohriak, W.U., 1999. Some remarks on the evolution of
746 sedimentary basins along the eastern Brazilian continental margin. *Episodes*
747 22, 206-216.

748 Calado, L., da Silveira, I.C.A., Gangopadhyay, A., de Castro, B.M. 2010. Eddy-
749 induced upwelling off Cape São Tomé (22 degrees S, Brazil). *Continental*
750 *Shelf Research* 30, 1181-1188.

751 Campos, E., Velhote, D., Silveira, I.C., 2000. Shelf-break upwelling driven by
752 Brazil Current cyclonic meanders. *Geophysical Research Letters* 27, 751-754.

753 Cattaneo, A., Steel, R.J.T., 2003. Transgressive deposits: a review of their
754 variability. *Earth-Science Reviews* 62, 187–228.

755 Catuneanu, O., 2006. *Principles of Sequence Stratigraphy*. Ed. Elsevier, 375 pp.

756 Chang, H.K., Kowsmann, R.O., Figueiredo, A.M.F., Bender, A., 1992. Tectonics
757 and Stratigraphy of the East Brazil Rift System: an Overview.
758 *Tectonophysics* 213, 97-138.

759 Clark, P.U., 2009. Ice sheet retreat and sea level rise during the last
760 deglaciation. *PAGES News* 17, 64-66.

- 761 Chappell, J., Shackleton, N.J. 1986. Oxygen isotopes and sea level. *Nature* 324,
762 137–140.
- 763 Corrêa, I.C.S., Ponzi, V.R.A., Trindade, L.A.F., 1980. Níveis marinhos
764 quaternários da plataforma continental do Rio de Janeiro. XXXI Cong. Bras.
765 Geologia, pp. 578-587 (in Portuguese).
- 766 Correa, I.C.S., 1996. Les variations du niveau de la mer durant les driers
767 17.500 ans BP: l'exemple de la plate-forme continentale du Rio Grande do
768 Sul – Brésil. *Marine Geology* 130, 163-178 (in French).
- 769 Costa, M.P.A., Alves, E.C., Pacheco, P.G., Maia, A.S., 1988. Prováveis
770 estabilizações do nível do mar holocênico em trechos da plataforma
771 continental entre o norte de São Paulo e o sul do Rio de Janeiro,
772 constatadas através de morfologia de detalhe. XXXV Cong. Bras. Geologia,
773 pp. 436-450 (in Portuguese).
- 774 Cutler, K.B., Edwards, R.L., Taylor, F.W., Cheng, H., Adkins, J., Gallup, C.D.,
775 Cutler, P.M., Burr, G.S., Bloom, A.L., 2003. Rapid sea-level fall and deep
776 ocean temperature change since the last interglacial period. *Earth and*
777 *Planetary Science Letters* 206, 253–271.
- 778 Duarte, C.S.L., Viana, A.R., 2007, Santos drift system: stratigraphic organization
779 and implications for late Cenozoic palaeocirculation in the Santos Basin, SW
780 Atlantic Ocean. In: Viana, A.R., Rebesco, M. (Eds.), *Economic and*
781 *palaeoceanographic significance of contourite deposits*. Geological Society of
782 London Special Publications 276, 171-198.
- 783 Duncan, C.S., Goffa, J.A., Austin Jr, J.A., Fulthorpe, C.S., 2000. Tracking the last
784 sea-level cycle: sea-floor morphology and shallow stratigraphy of the latest
785 Quaternary New Jersey middle continental shelf. *Marine Geology* 170, 395-
786 421.
- 787 Emery, K.O., Uchupi, E., 1984. *The Geology of the Atlantic Ocean*. Springer, New
788 York, 1050 pp.
- 789 Fairbanks, R.G., 1989. A 17,000-year glacio-eustatic sea level record: influence
790 of glacial melting dates on the Younger Dryas event and deep-ocean
791 circulation. *Nature* 342, 637–642.
- 792 Fernández-Salas, L.M., Dabrio, C.J., Goy, J.L., Díaz Del Río, V., Zazo, C., Lobo,
793 F.J., Sanz, J.L., Lario, J., 2009. Land–sea correlation between Late
794 Holocene coastal and infralittoral deposits in the SE Iberian Peninsula
795 (Western Mediterranean). *Geomorphology* 104, 4–11.

796 Figueiredo Jr, A.G., Tessler, M.G., 2004. Topografia e composição do substrato
797 marinho da Região Sudeste-Sul do Brasil. Technical Report, Instituto
798 Oceanográfico (USP). Série Documentos Revizee – Score Sul, 64 pp. São
799 Paulo, Brazil (in Portuguese).

800 Friederichs, Y.L., Reis, A.T., Silva, C.G., Toulemonde, B., Maia, R.M.C, Guerra,
801 J.V., in press. The seismic architecture of the Sepetiba fluvio-estuarine
802 system preserved on the shallow stratigraphic record on the offshore inner-
803 mid shelf, Rio de Janeiro, Brazil. Revista Brasileira de Geociências (in
804 Portuguese).

805 Hernandez-Molina, F.J., Fernández-Salas, L.M., Lobo, F.J., Somoza, L., Díaz Del
806 Río, V., Alveirinho Dias, J.M., 2000. The infralittoral prograding wedge: a
807 new large-scale progradational sedimentary body in shallow marine
808 environments. *Geo-Marine Letters* 20, 109–117.

809 Imbrie, J., Hays, J.D., Martinson, D.G., McIntyre, A., Mix, A.C., Morley, J.J.,
810 Pias, N.G., Prell, W.L., Shackleton, N.J., 1984. The orbital theory of
811 Pleistocene climate: support from a revised chronology of the marine $\delta^{18}O$
812 record. In: Berger, A., Imbrie, J., Hays, J., Kukla, G., Saltzman, B. (Eds.),
813 Milankovitch and climate. Reidel Publishing Company, Dordrecht, pp. 269–
814 305.

815 Kowsmann, R.O., Costa, M.P.A., Vicalvi, M.A., Coutinho, M.G.M., Gamboa, L.A.P.,
816 1977. Modelo da sedimentação holocênica na plataforma continental sul
817 brasileira. In: Projeto REMAC – Evolução sedimentar holocênica da
818 plataforma continental e do talude do Sul do Brasil. Série Projeto REMAC,
819 PETROBRAS, CENPES-DINTEP, 2, pp. 7–26 (in Portuguese).

820 Kowsmann, R., Vicalvi, M., Costa, M., 1979. Considerações sobre a sedimentação
821 quaternária na plataforma continental entre Cabo Frio e o rio Itabapoana.
822 *Notícia Geomorfológica* 19 (37-38), 41-58 (in Portuguese).

823 Kowsmann, R.O., Costa, M.O.A., 1979. Sedimentação quaternária da margem
824 continental brasileira e das áreas oceânicas adjacentes. Série Projeto
825 REMAC, PETROBRAS, CENPES-DINTEP Petrobrás, Rio de Janeiro, 55 pp (in
826 Portuguese).

827 Labeyrie, L.D., Duplessy, J.C., Blanc, P.L., 1987. Variations in mode of formation
828 and temperature of oceanic deep waters over the past 125.000 years.
829 *Nature* 327, 477–482.

830 Lambeck, K., 1997. Sea-level change along the French Atlantic and Channel
831 coasts since the time of the Last Glacial Maximum. *Palaeogeography,*
832 *Palaeoclimatology and Palaeoecology* 129, 1–22.

833 Lambeck, K., Bard, E., 2000. Sea-level change along the French Mediterranean
834 coast from the past 30000 years. *Earth and Planetary Science Letters* 175,
835 203–222.

836 Lambeck, K., Chappell, J., 2001. Sea level change through the Last Glacial Cycle.
837 *Science* 292, 679–686.

838 Lambeck, K., Yokoyama, Y., Purcell, A., 2002. Into and out of the Last Glacial
839 Maximum: sea-level change during the Oxygen Isotope 3 and 2. *Quaternary*
840 *Science Reviews* 21, 343–360.

841 Lambeck, K., Antonioli, F., Purcell, A., Silenzi, S., 2004. Sea-level change along
842 the Italian coast for the past 10,000 yr. *Quaternary Science Reviews* 23,
843 1567–1598.

844 Lobo, F.J., Sánchez, R., González, R., Dias, J.M.A., Hernández-Molina, F.J.,
845 Fernández-Salas, L.M., Díaz del Río, V., Mendes, I., 2004. Contrasting
846 styles of the Holocene highstand sedimentation and sediment dispersal
847 systems in the northern shelf of the Gulf of Cadiz. *Continental Shelf*
848 *Research* 24, 461-482.

849 Mahiques, M.M, da Silveira, I.C.A., Sousa, S.H.M., Rodrigues, M., 2002. Post-
850 LGM sedimentation on the outer shelf-upper slope of the northernmost part
851 of the São Paulo Bight, southeastern Brazil. *Marine Geology* 181, 387–400.

852 Mahiques, M.M, Tessler, M.G, Ciotti, A.M, Silveira, I.C.A., Sousa, S.H.M.,
853 Figueira, R.C.L, Tassinari, C.C.G., Furtado, V.V., Passos, R.F., 2004.
854 Hydrodynamically driven patterns of recent sedimentation in the shelf and
855 upper slope off Southeast Brazil. *Continental Shelf Research* 24, 1685-1697.

856 Mahiques, M.M, Bicego, M.C, Silveira, I.C.A, Sousa, S.H.M., Lourenço, R.A.,
857 Fukumoto, M.M., 2005. Modern sedimentation in the Cabo Frio upwelling
858 system, Southeastern Brazilian shelf. *Anais da Academia Brasileira de*
859 *Ciências* 77, 535-548.

860 Mahiques, M. M.; Fukumoto, M. M.; Silveira, I. C. A.; Figueira, R. C. L.; Bicego,
861 M. C.; Lourenço, R.A.; Sousa, S.H.M., 2007. Sedimentary changes on the
862 Southeastern Brazilian upper slope during the last 35 000 years. *Anais da*
863 *Academia Brasileira de Ciências* 79, 171-181.

864 Mahiques, M.M., Mello e Sousa, S.H., Furtado, V. V., Tessler, M.G., Toledo,
865 F.A.L., Burone, L., Figueira, R.C.L., Klein, D.A., Martins, C. C., Alves,

866 D.P.V., 2010. The Southern Brazilian shelf: general characteristics,
867 quaternary evolution and sediment distribution. *Brazilian Journal of*
868 *Oceanography* 58 (no.spe2), 25-34.

869 Maia, R.M.C., Reis, A.T., Alves, E.C., Silva, C.G., Guerra, J.V., Gorini, C., Silva,
870 A., Arantes-Oliveira, R., 2010. Architecture and stratigraphic framework of
871 shelf sedimentary systems off Rio de Janeiro state, northern Santos basin-
872 Brazil. *Brazilian Journal of Oceanography* 58 (no.spe2), 15-29.

873 Milliman, J.D., 1978. Morphology and structure of the upper continental margin
874 of Southern Brazil. *Bulletin of the American Association of Petroleum*
875 *Geologists* 62, 1029-1048.

876 Milliman, J.D., Jiezao, Z., Anchun, L., Ewing, J., 1990. Late Quaternary
877 sedimentation on the outer and middle New Jersey continental shelf: result
878 of two local deglaciations? *Journal of Geology* 98, 966-976.

879 Mitchum, R.M. Jr., Vail, P.R., Sangree, J.B., 1977a. Seismic stratigraphy and
880 global changes of sea level; Part 6, Stratigraphic interpretation of seismic
881 reflection patterns in depositional sequences. In: *Seismic Stratigraphy:*
882 *Application to Hydrocarbon Exploration*. American Association of Petroleum
883 Geologists Memoir 26, 117-133.

884 Mitchum, R.M., Vail, P.R., Sangree, J.B., 1977b. Seismic stratigraphy and global
885 changes of sea level, part 7: Seismic stratigraphy interpretation
886 procedures. In: Payton, C.E. (Ed.), *Seismic Stratigraphy: Application to*
887 *Hydrocarbon Exploration*. American Association of Petroleum Geologists
888 Memoir 26, 135-143.

889 Modica, C.J.; Brush, E.R., 2004. Post-rift sequence stratigraphy, paleogeography,
890 and fill history of the deep-water Santos Basin, offshore southeast Brazil.
891 *Bulletin of the American Association of Petroleum Geologists* 88, 923-945.

892 Nagai, R.H., Mello e Sousa, S.H., Lourenço, R.A., Bícigo, M.C., Mahiques, M.M.,
893 2010. Paleoproductivity changes during the late Quaternary in the
894 southeastern Brazilian upper continental margin of the southwestern
895 Atlantic. *Brazilian Journal of Oceanography* 58 (no.spe2), 31-41.

896 Plint, A.G., Nummedal, D., 2000. The falling stage systems tract: recognition and
897 importance in sequence stratigraphy. In: Hunt, D., Gawthorpe, R.L. (Eds.),
898 *Sedimentary responses to forced regressions*. Geological Society of London,
899 pp. 1-17.

900 Rabineau, M., Berné, S., Aslanian, D., Olivet, J.L., Joseph, P., Guillocheau, F.,
901 Bourillet, J.F., Ledrezen, E., Granjeon, D., 2006. Paleo sea levels

902 reconsidered from direct observation of paleoshoreline position during
903 Glacial Maxima (for the last 500,000 yr). *Earth and Planetary Science*
904 *Letters* 252, 119–137.

905 Rocha, J., Milliman, J.D., Santana, C.I., Vicalvi, M.A., 1975. Continental margin
906 sedimentation off Brazil Part 5: Southern Brazil. *Contributions to*
907 *Sedimentology* 4, 117–150.

908 Rodrigues, R.R., Lorenzetti, J.A., 2001. A numerical study of the effects of
909 bottom topography and coastline geometry on the Southeast Brazilian
910 coastal upwelling. *Continental Shelf Research* 21, 371-394.

911 Rohling, E.J., Fenton, M., Jorissen, F.J., Bertrand, P., Ganssen, G., Caulet, J.P.,
912 1998. Magnitudes of sea level lowstands of past 500,000 years. *Nature*
913 394, 162–165.

914 Schattner, U., Lazar, M., Tibor, G., Ben-Avraham, Z., Makovsky, Y., 2010. Filling
915 up the shelf — A sedimentary response to the last post-glacial sea rise.
916 *Marine Geology* 278, 165–176

917 Shackleton, N.J., 2000. The 100,000-year Ice-Age cycle identified and found to
918 lag temperature, carbon dioxide, and orbital eccentricity. *Science* 289,
919 1897-1902.

920 Siddall, M., Almogi-Labin, R.E. J. A., Hemleben, C., Meischner, D., Schmelzer, I.,
921 Smeed, D.A., 2003. Sea-level fluctuations during the last glacial cycle.
922 *Nature* 423, 853–858.

923 Signorini, S.R., 1978. On the circulation and the volume transport of the Brazil
924 Current between the Cape of São Tomé and Guanabara Bay. *Deep-Sea*
925 *Research* 25, 481-490.

926 Silveira, I.C, Schmidt, A., Campos, E., Godoi, S., Ikeda, Y., 2000. A corrente do
927 Brasil ao largo da costa leste brasileira. *Revista Brasileira de Oceanografia*.
928 48, 171-183 (in Portuguese).

929 Skene, K.I., Piper, D.J.W., Aksu, A.E., Syvitski, J.P.M., 1998. Evaluation of the
930 global oxygen isotope curve as a proxy for Quaternary sea level by
931 modeling of delta progradation. *Journal of Sedimentary Research* 68, 6,
932 1077–1092.

933 Smith, W.H.F, Sandwell, D.T., 1997. Global Seafloor topography from satellite
934 altimetry and ship depth soundings. *Science* 227, 1956-1962.

935 Soutelino, R.G., 2008. A origem da corrente da Brasil. 2008. Master dissertation,
936 Instituto Oceanográfico. Universidade of São Paulo (USP), São Paulo, Brazil
937 (in Portuguese).

938 Stanley, D.J., Moore, G.T., 1983. The shelfbreak: critical interface on continental
939 margins. Society of Economic Paleontologist and Mineralogist Special
940 Publication 33, 467 pp.

941 Stramma, L., England, M., 1999. On the water masses and mean circulation of
942 the South Atlantic Ocean. Journal of Geophysical Research 104 (C9),
943 20863-20883.

944 Szabo, B.J., Ludwig, K.R., Muhs, D.R., Simmons, K.R., 1994. Thorium- 230 ages
945 of corals and duration of the last interglacial sea-level high stand on Oahu,
946 Hawaii. Science 266, 93–96.

947 Toscano, M.A., Lundberg, J., 1999. Submerged Late Pleistocene reefs on the
948 tectonically-stable SE Florida margin: high precision geochronology,
949 stratigraphy, resolution of Substage 5a sea-level elevation, and orbital
950 forcing. Quaternary Science Reviews 18, 753–767.

951 Waelbroeck C., Labeyrie L.D., Michel E., Duplessy J.-C., McManus, J. Lambeck
952 K., Balbon E., Labracherie M., 2002. Sea level and deep water changes
953 derived from benthic Foraminifera isotopic record, Quaternary Science
954 Reviews 21, 295–305.

955 Zalán P.V., Oliveira J.A.B., 2005. Origem e evolução estrutural do Sistema de
956 Riftes Cenozóicos do Sudeste do Brasil. Boletim de Geociências da Petrobras
957 13, 269-300 (in Portuguese).

958 Zemruscki, S.G., 1979. Geomorfologia da margem continental sul-brasileira e
959 das bacias oceânicas adjacentes. In: Chaves, H.A.F. (Ed.). Geomorfologia
960 da margem continental brasileira e das bacias oceânicas adjacentes. Projeto
961 REMAC 7. Petrobrás, Rio de Janeiro, pp 129-177 (in Portuguese).

962
963
964

965 **FIGURE CAPTION**

966

967 **Figure 1:** Regional bathymetry of the continental shelf off Rio de Janeiro State,
968 northern Santos basin, with location of the study area, tracklines of single-
969 channel seismic data and exploratory wells. Regional bathymetry from ETOPO2
970 ([Smith and Sandwell, 1997](#)).

971

972 **Figure 2:** Distribution of surface sediments in the study area. Redrawn from
973 [Figueiredo and Tessler \(2004\)](#) over ETOPO2 regional bathymetry ([Smith and](#)
974 [Sandwell, 1997](#)).

975

976 **Figure 3:** (A) Interpreted dip single-channel seismic line (sparker 1000 J) across
977 the eastern shelf sector off Rio de Janeiro State, illustrating a lower
978 aggradational-progradational stratigraphic Set I and Set II (modified from [Maia](#)
979 [et al., 2010](#); Set II encompasses Middle-Upper Pleistocene deposition: last ~440-
980 500 Kyr). (B) Sequence boundaries S1 to S5, topping successive 4th order
981 sequences Sq1 to Sq4. Sq5 corresponds to Holocene transgressive and highstand
982 deposition from the current half-cycle (post-LGM). Note offlapping distal oblique
983 clinoforms within Sq2 to Sq4, showing significant stepped morphology, imprinted
984 on respective palaeo-sea-floors and the present shelf sea floor. (C) Proposed
985 depositional cyclicity based on correlation with $\delta^{18}\text{O}$ -derived global sea level
986 variations compiled by [Rabineau et al. \(2006\)](#).

987

988 **Figure 4:** Serial bathymetric cross-sections aligned roughly N-S, showing
989 progressive east-west changes in morphology and width of the continental shelf
990 off southern Rio de Janeiro State. Bathymetric data are a compilation of over 50
991 years of bathymetric sounding charts acquired by the Brazilian Navy.

992

993 **Figure 5:** Shelf morphological map off southern Rio de Janeiro State,
994 highlighting shelf-scale contour-parallel sea-floor features, mapped with the aid
995 of high-resolution seismic analysis and bathymetric data. Dotted thick lines
996 represent buried escarpments. Features 1 to 9 are discussed in the text.

997

998 **Figure 6:** Conjugated bathymetric and seafloor gradient map off southern Rio de
999 Janeiro State. Bathymetric data are a compilation of over 50 years of
1000 bathymetric sounding charts acquired by the Brazilian Navy, made available by
1001 CHM-Centro Hidrográfico da Marinha do Brasil.

1002

1003 **Figure 7:** Sub-bottom dip profile (frequency chirp ~0,5-5,5 kHz, top) and
1004 interpreted line drawing (bottom) across the central shelf sector off Rio de
1005 Janeiro State. Chirp profiles revealed further architectural detail in the upper
1006 sequences (Sq3 to Sq5), originating from alternating marine deposition and
1007 subaerial erosion encompassing the last few Quaternary climate cycles

1008 (presumably the youngest 230-250 kyr). (T-R) Composite transgressive-
1009 regressive wedge, (Tr) Transgressive units, (Hs) Highstand units, (FSST) Falling-
1010 stage Systems Tract, (HST) Highstand Systems Tract, (S3-S5) Unconformities,
1011 (E) Sea-floor escarpments.

1012

1013 **Figure 8:** Extracts of sub-bottom cross-section profiles (frequency chirp ~0,5-
1014 5,5 kHz) extending over the mid-outer shelf seaward from the ~100-m isobath.
1015 The -110 m and -130 m laterally-continuous sea-floor escarpments are erosive
1016 imprints of S5 lowstand exposure surface. The distal escarpment at -150 m
1017 water depth, and associated seaward-inclined basal terrace, shows evidence of
1018 accentuated erosion, probably in response to contour currents. (E) Sea-floor
1019 escarpments, (Tr) Transgressive units, (FRw) Forced-regressive wedges, (S1-S5)
1020 Unconformities.

1021

1022 **Figure 9:** Extracts of sub-bottom cross-sections (A and B) and sparker seismic
1023 lines, located at the shelfbreak along the western shelf-edge embayment,
1024 showing the lateral variability of the -150 m escarpment (E) and basal seaward-
1025 inclined terrace. (Cr) Carbonate bioconstructions.

1026

1027 **Figure 10:** Envelope of sea-level curves based on $\delta^{18}\text{O}$ isotopic ratio's and
1028 calibrated by the dating of geological evidence globally (see text and references),
1029 and correlation of the S4 and S5 unconformities in the study area to it.

1030

1031 **Figure 11:** Sub-bottom strike profile (frequency chirp ~0,5-5,5 kHz; top) and
1032 interpreted line drawing (bottom) across the outer shelf off southern Rio de
1033 Janeiro State. Overall thickness reduction of sequences Sq3 and Sq4 within the
1034 shelf corridors evidence the significant erosion forming these elongated
1035 depressions across the mid-outer shelf (see Figs. 5 and 15 for plan views). (Tr)
1036 Transgressive units, (FSST) Falling-Stage Systems Tract, (S3-S5) named
1037 unconformities.

1038

1039 **Figure 12:** Sub-bottom dip profile (frequency chirp ~0,5-5,5 kHz; top) and
1040 interpreted line drawing (bottom) crossing the Western Shelf Corridor. This
1041 particular section shows sequence Sq4 to be deeply eroded so that erosional
1042 surfaces S5 and S4 have merged over most of the mid-outer shelf, leaving a a
1043 composite and smooth-topped erosional surface that apparently obliterated the

1044 morphological relief of the -110m and -130m escarpments. (Tr) Transgressive
1045 units, (FSST) Falling-stage Systems Tract, (S3-S5) Unconformities, (E) Sea-floor
1046 escarpments.

1047

1048 **Figure 13:** Extracts of sub-bottom cross-section profiles (frequency chirp ~0,5-
1049 5,5 kHz) located landward from the 100-m isobath, showing east-west
1050 differences in inner-mid shelf morphology and architecture, with westward higher
1051 preservation of young composite transgressive and highstand features (Sq5), in
1052 relation to such feature preservation for next-older sequence (Sq4) and bounding
1053 erosion surfaces (S4, S5).

1054

1055 **Figure 14:** Extracts of sub-bottom profiles (frequency chirp ~0,5-5,5 kHz)
1056 showing carbonate bioconstructions, locally as thick as 10 m, to be widespread
1057 across areas of the mid-outer shelf seaward from the 100-m isobath.

1058

1059 **Figure 15:** Simplified geomorphological map of the continental shelf off southern
1060 Rio de Janeiro State linking high-resolution seismic analysis with the occurrence
1061 of laterally-continuous drowned sea-floor features resulting from Late Pleistocene
1062 sea level oscillations (i.e. in the last ~120 kyr). Dotted thick lines represent
1063 buried escarpments.

1064

1065 **Figure 16:** Simple conceptual stratigraphic model relating the origin of linear,
1066 stepped sea-floor features along the continental shelf off Rio de Janeiro State to
1067 the eustatic sea-level (SL) regressive scenario between MIS5e and MIS2 (Late
1068 Pleistocene). The inset curve is derived from [Labeyrie et al. \(1987\)](#), with T-R =
1069 Composite transgressive-regressive wedge and FSST = Falling-stage Systems
1070 Tract: (A-D) sediments related to the older part of the cycle, when sea-level was
1071 still relatively high are deposited on the inner shelf, with several subunits that
1072 may be related to higher frequency sea-level oscillations (MIS 5e-5a and MIS 4);
1073 (E-F) sediments related to the younger part of the regressive cycle (MIS 3 to MIS
1074 2) are deposited as forced regressive sequences on the outer shelf. The -110 m
1075 escarpment is sculpted between MIS 3 and MIS 2 (between **t4** and **t6**). The -130
1076 m escarpment relates to the LGM shoreline (at **t6**); (G) The -150 m scarp marks
1077 enhanced erosion due to shelfward migration of the Brazil Current during the
1078 post-LGM transgression (between **t6** and **t7**).

Figure1

[Click here to download high resolution image](#)

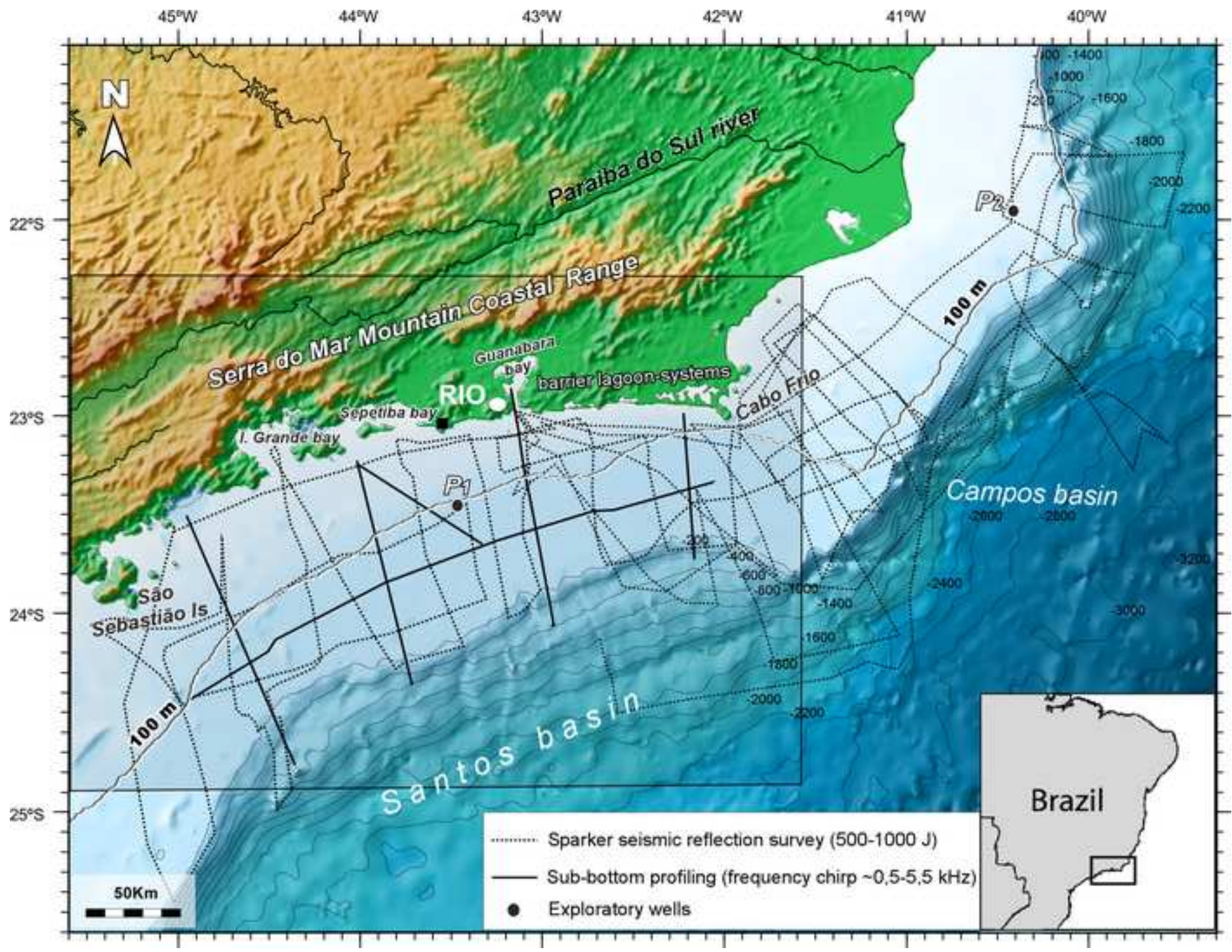


Figure2

[Click here to download high resolution image](#)

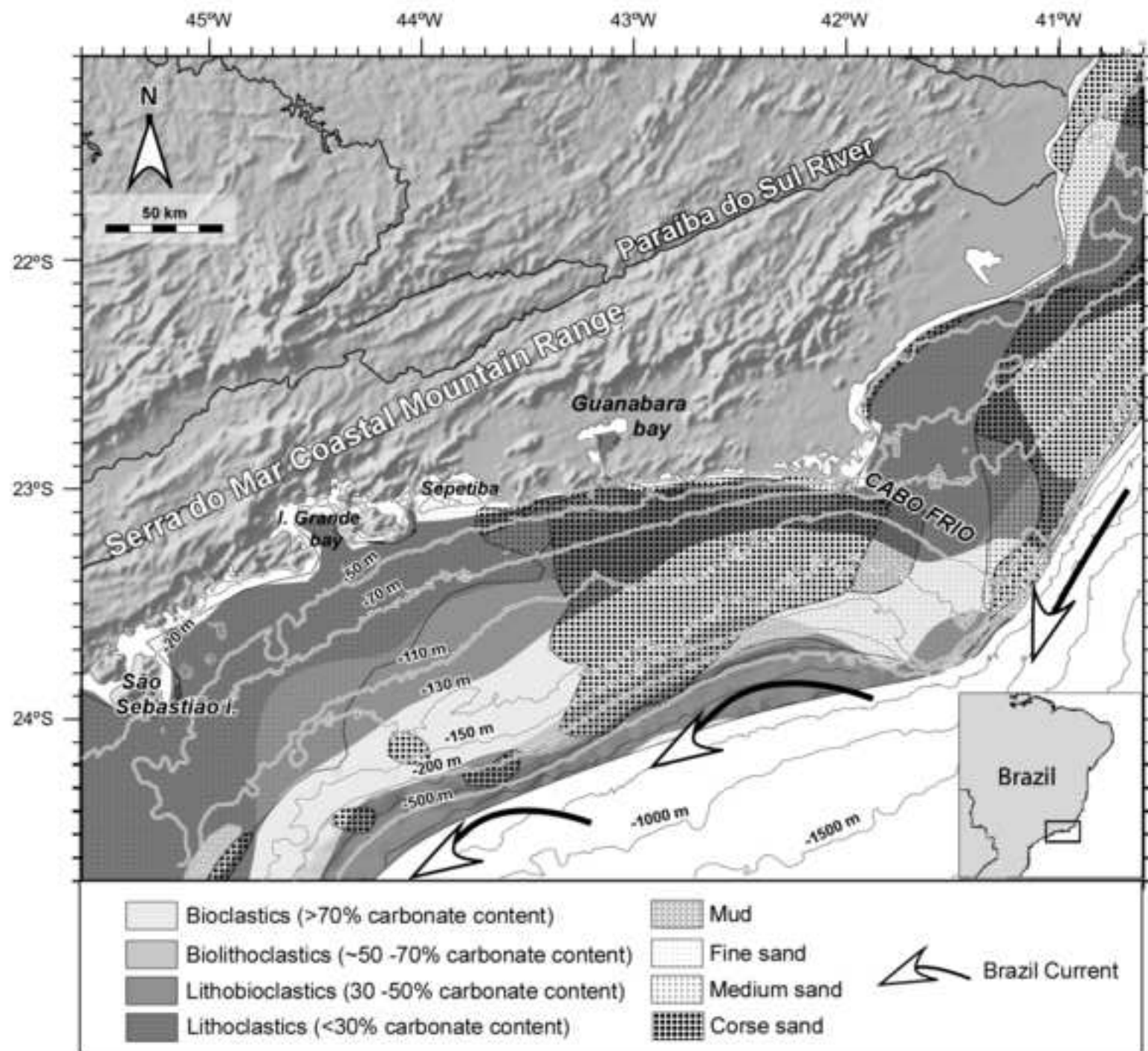


Figure3

[Click here to download high resolution image](#)

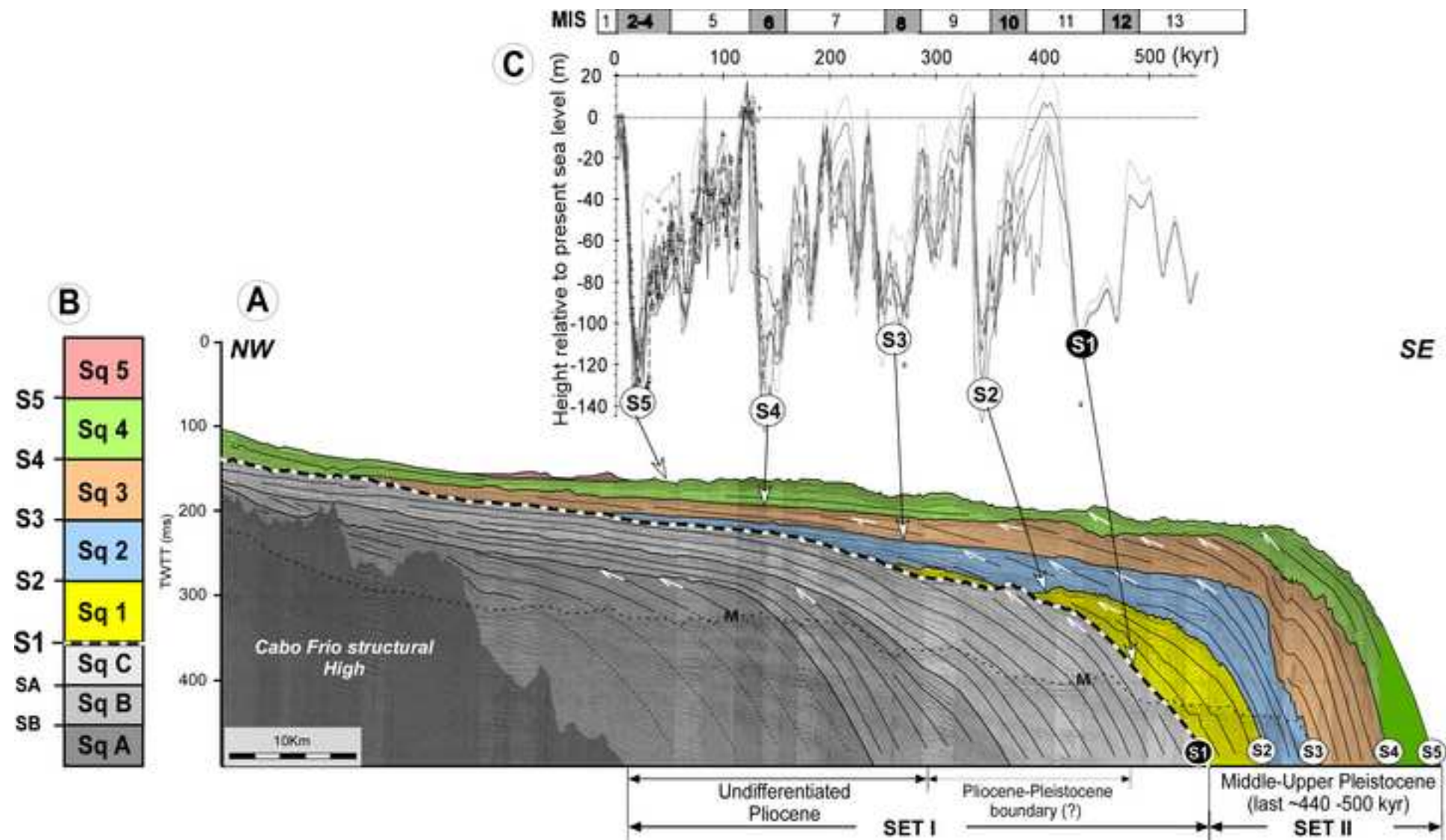


Figure 4

[Click here to download high resolution image](#)

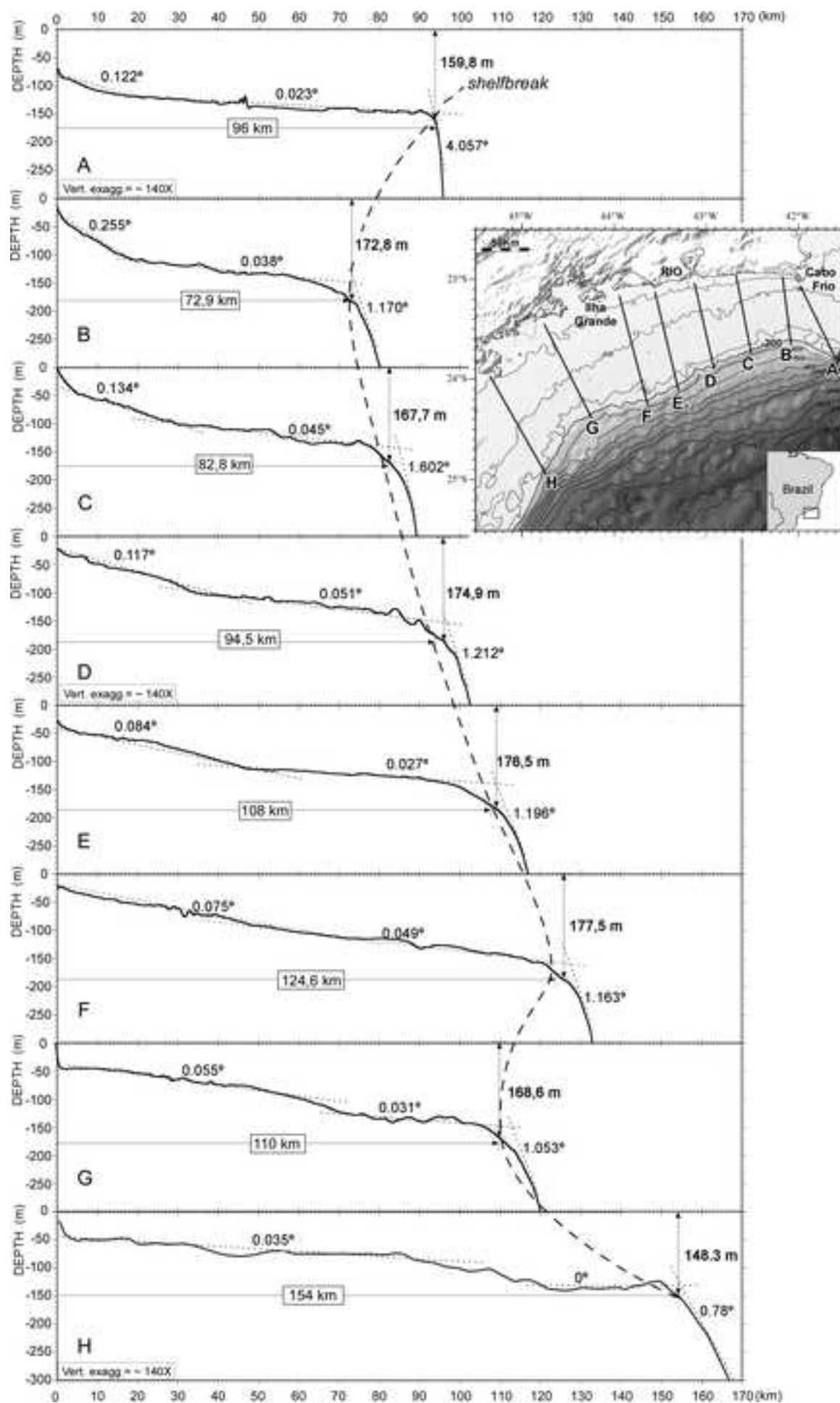


Figure 5

[Click here to download high resolution image](#)

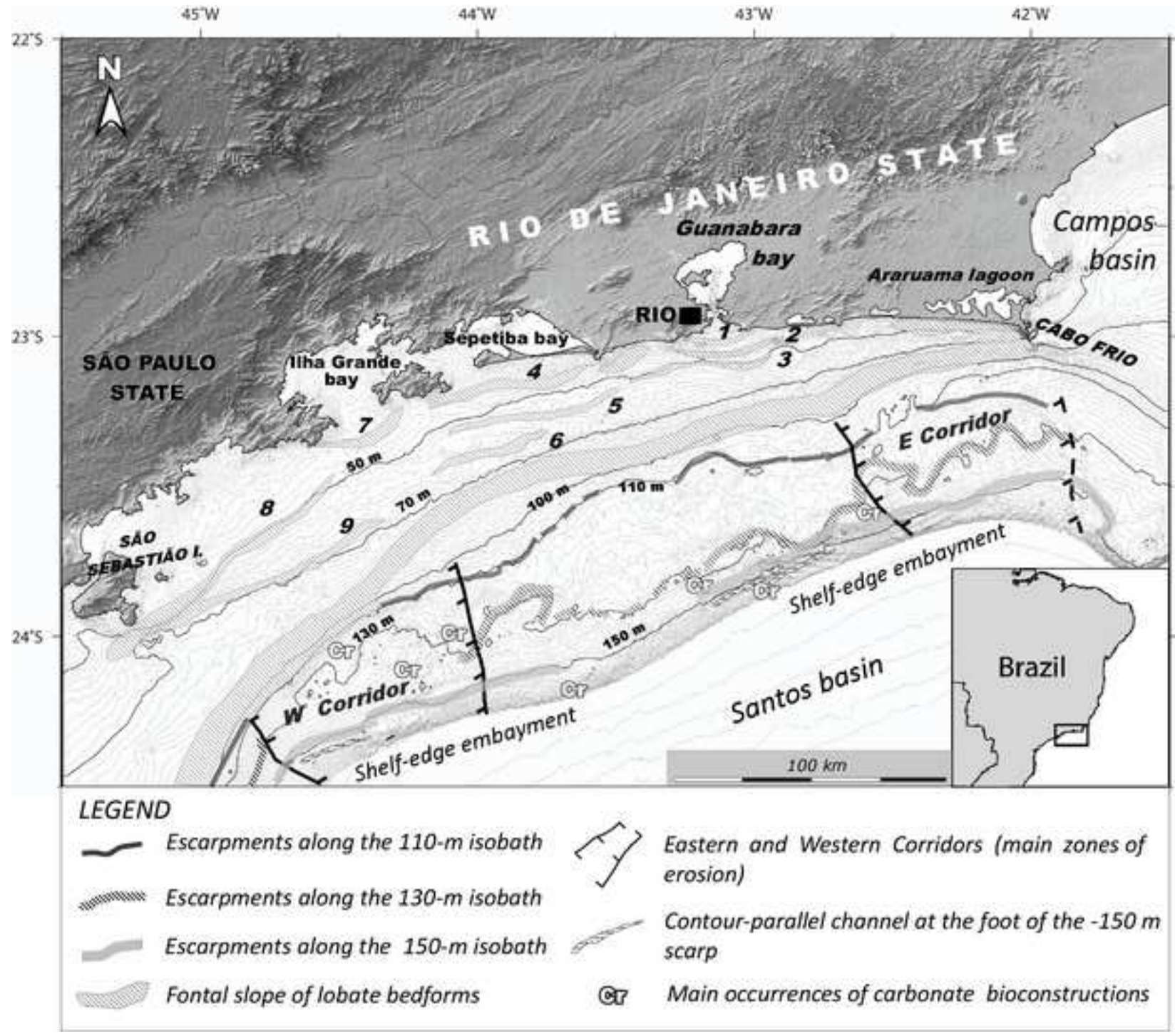


Figure6
[Click here to download high resolution image](#)

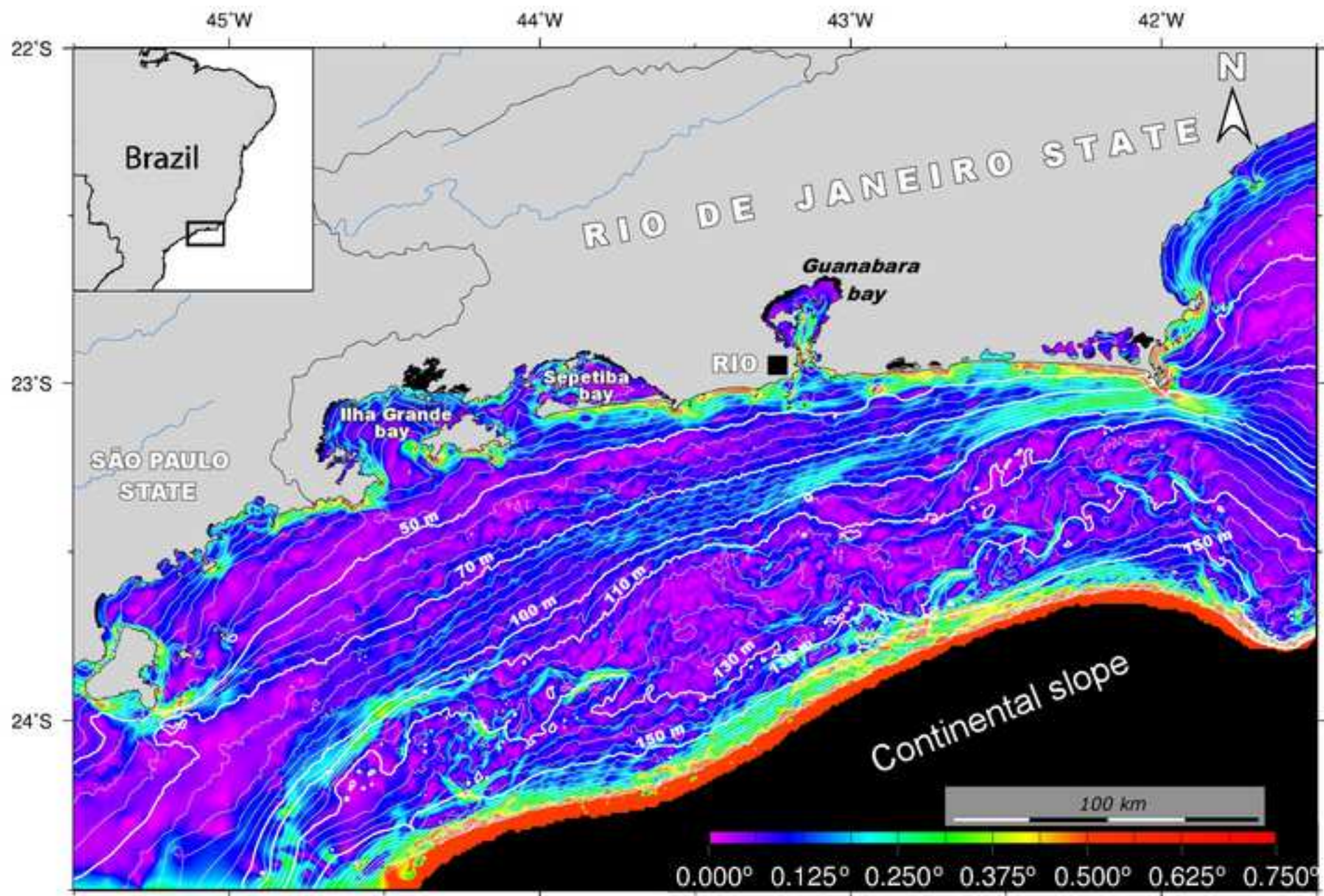


Figure7
[Click here to download high resolution image](#)

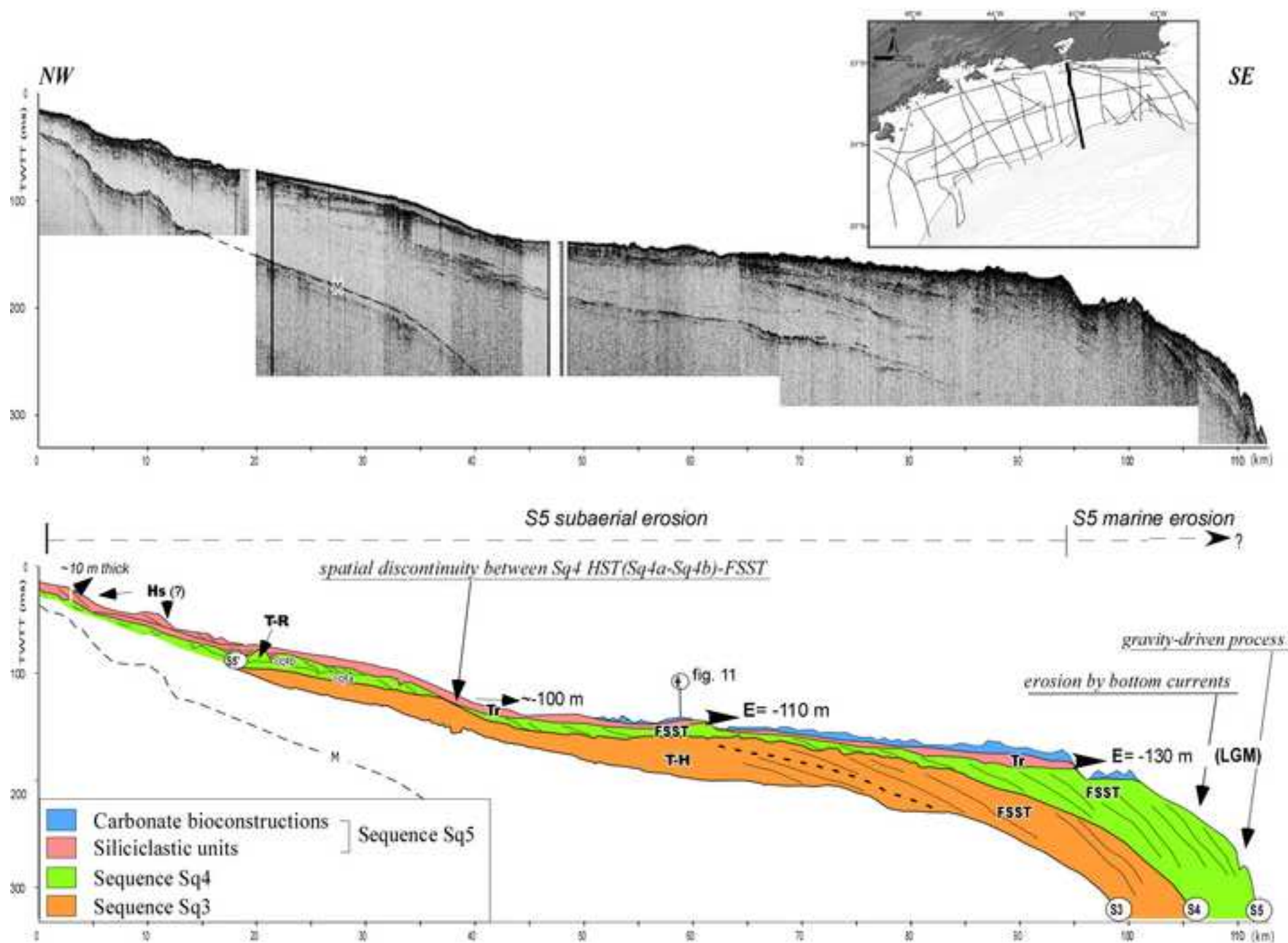


Figure8

[Click here to download high resolution image](#)

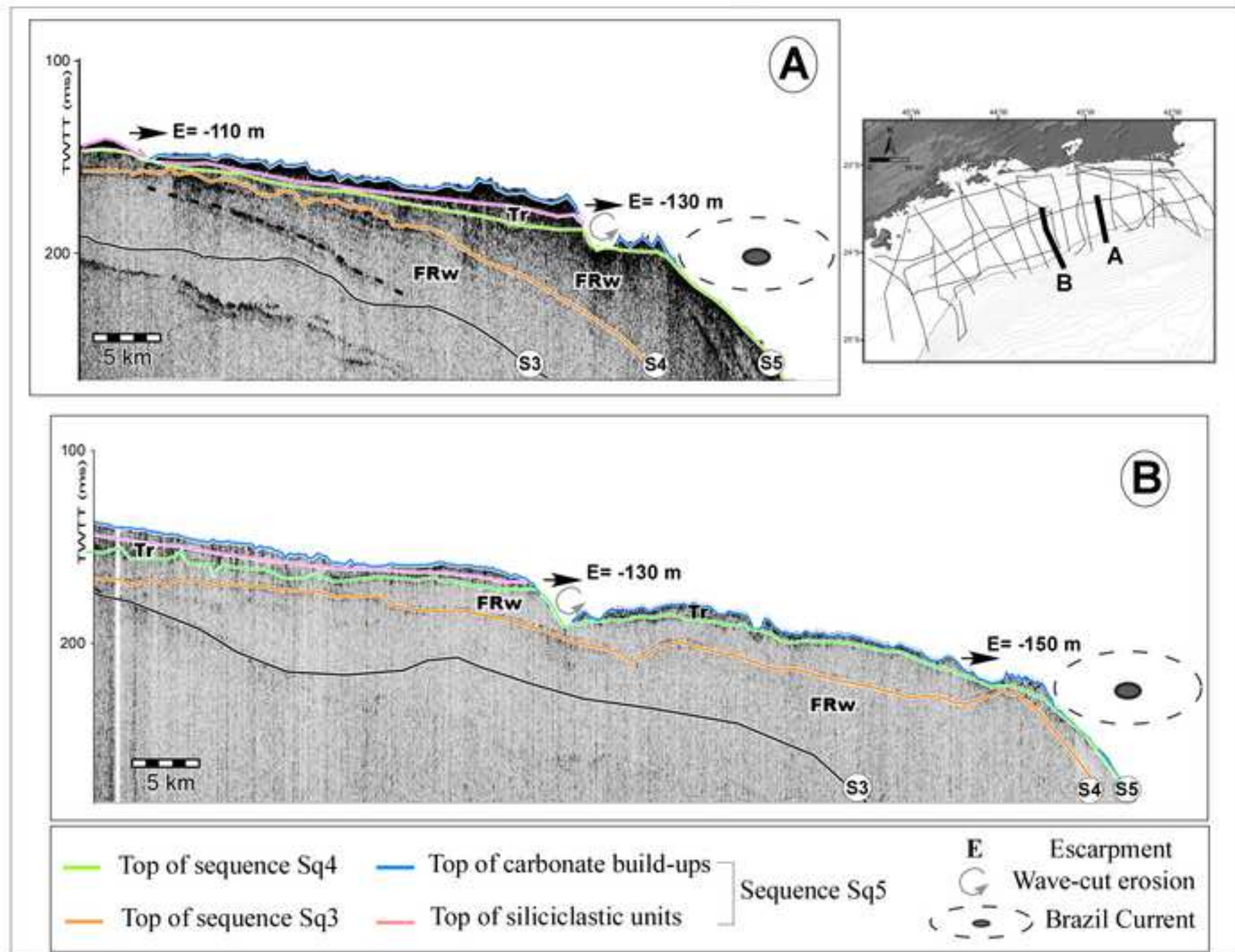


Figure9

[Click here to download high resolution image](#)

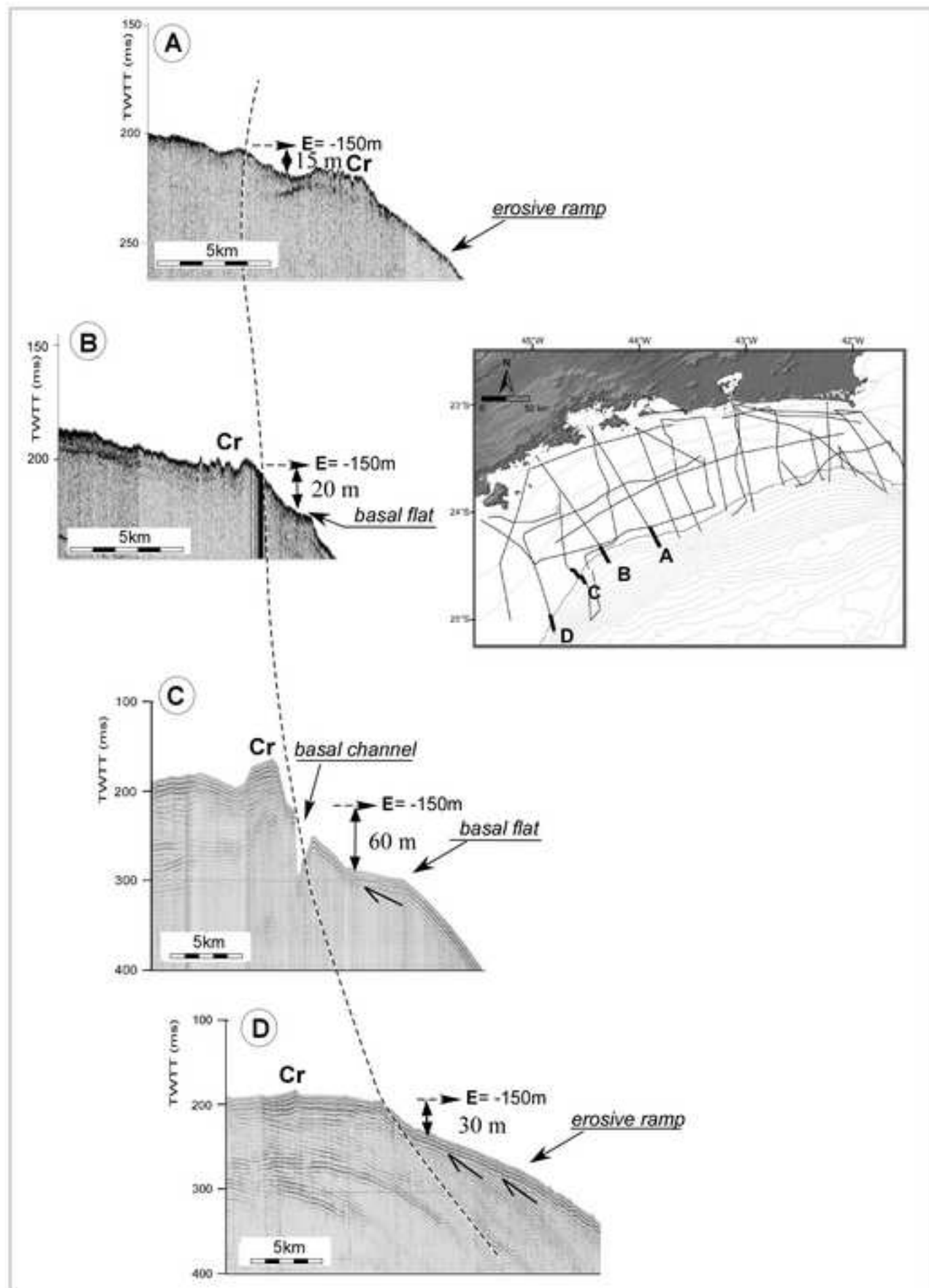


Figure10

[Click here to download high resolution image](#)

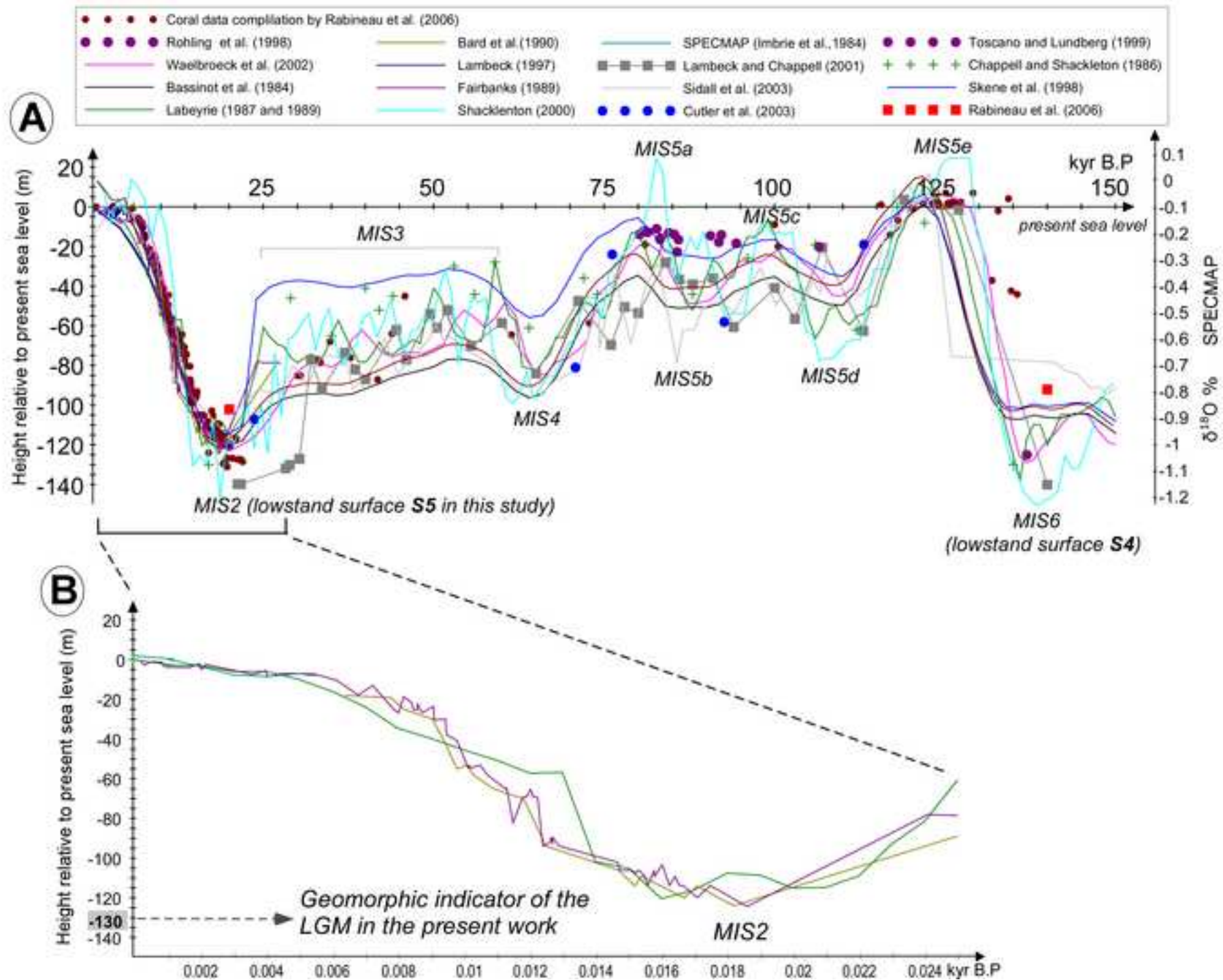


Figure11
[Click here to download high resolution image](#)

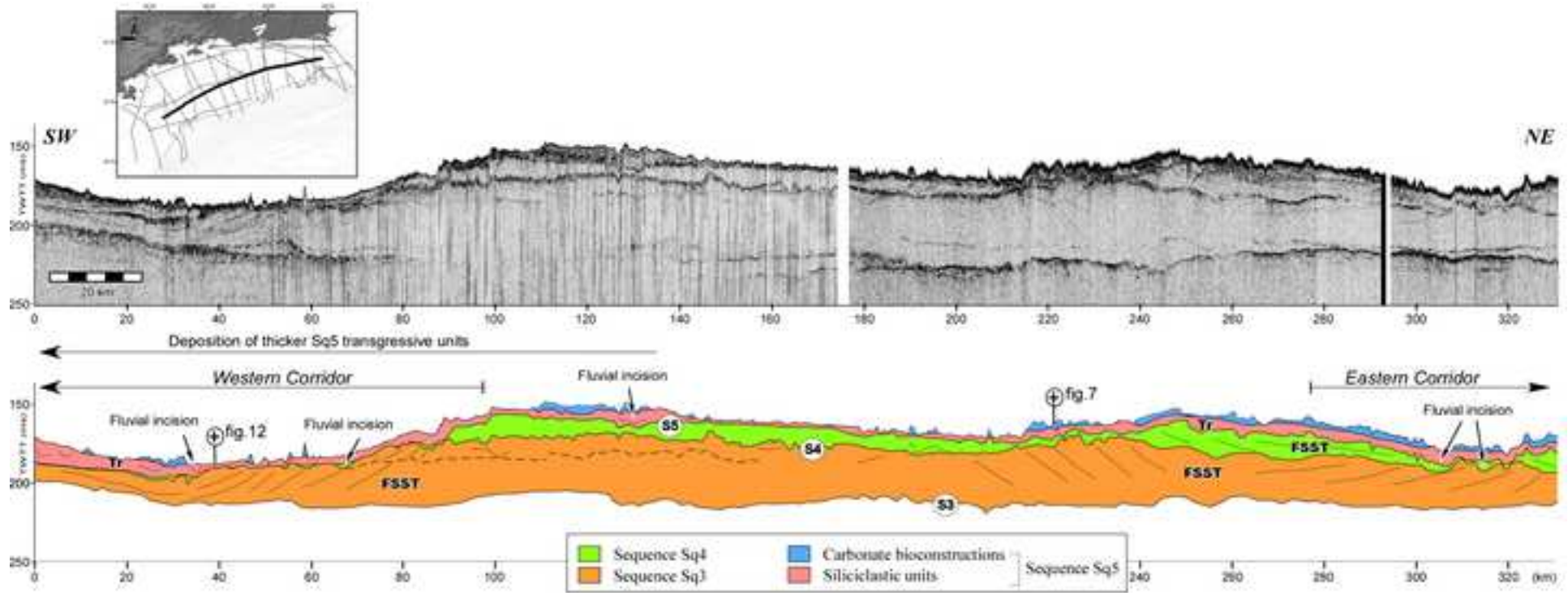


Figure12

[Click here to download high resolution image](#)

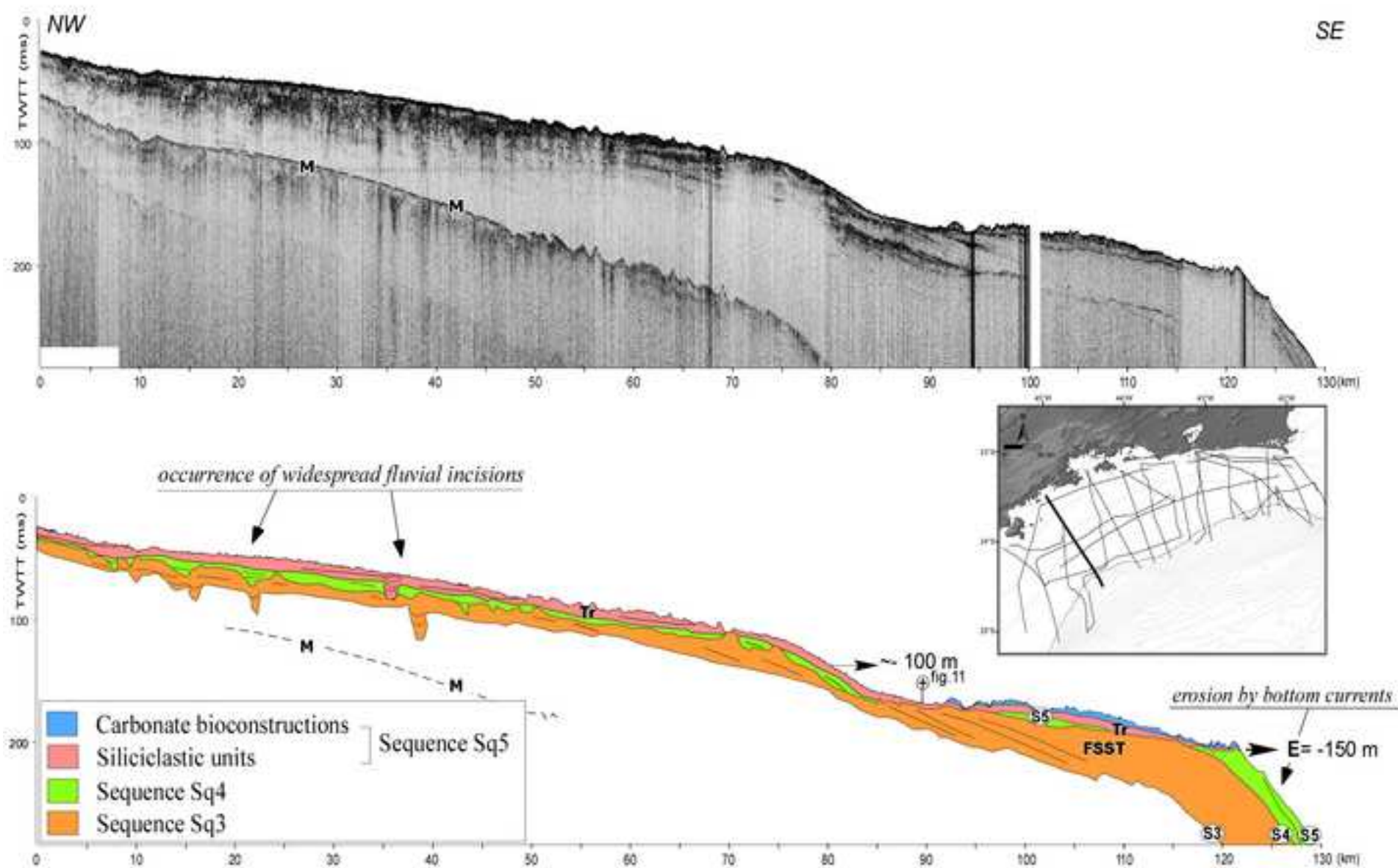


Figure13

[Click here to download high resolution image](#)

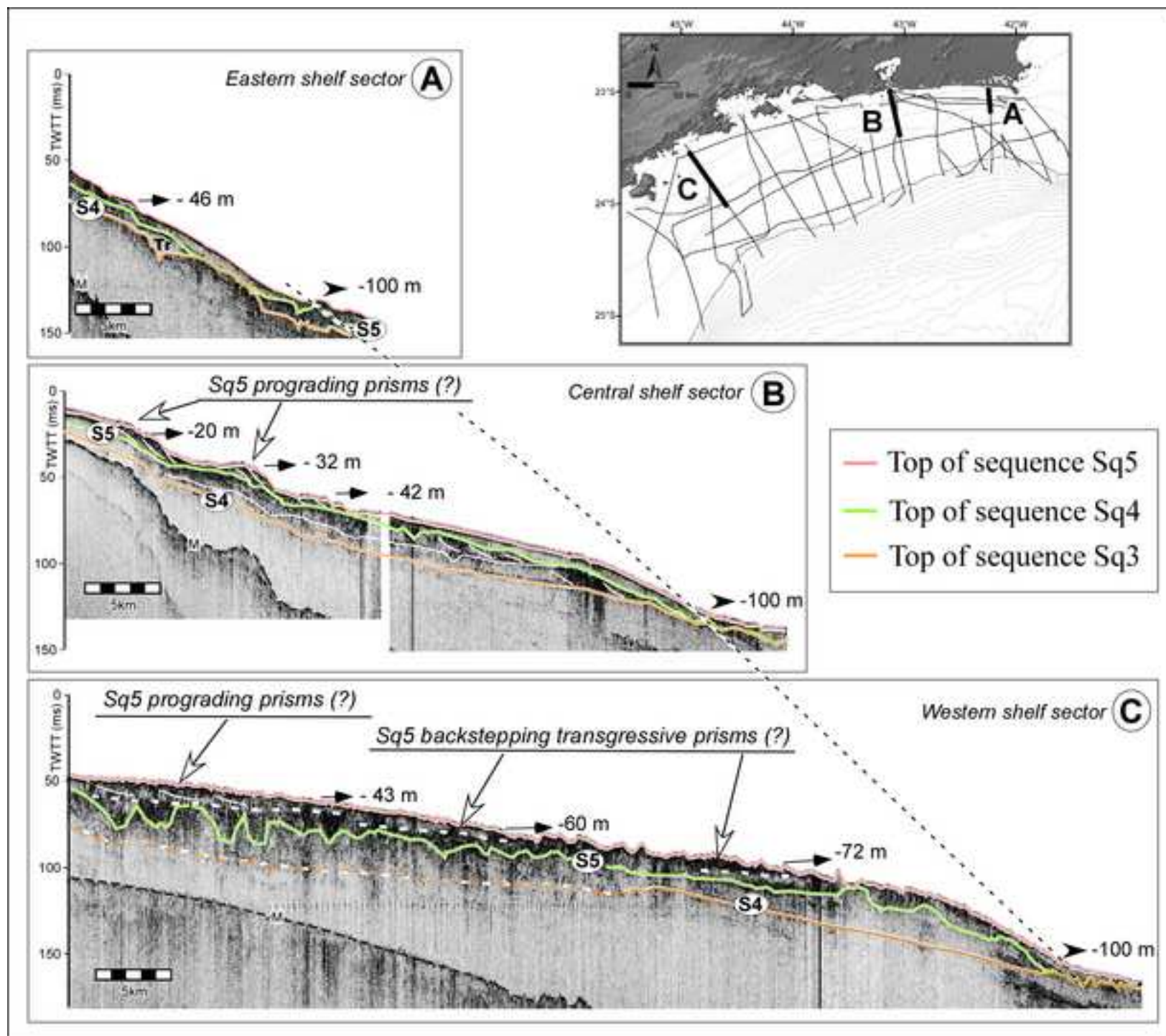


Figure14

[Click here to download high resolution image](#)

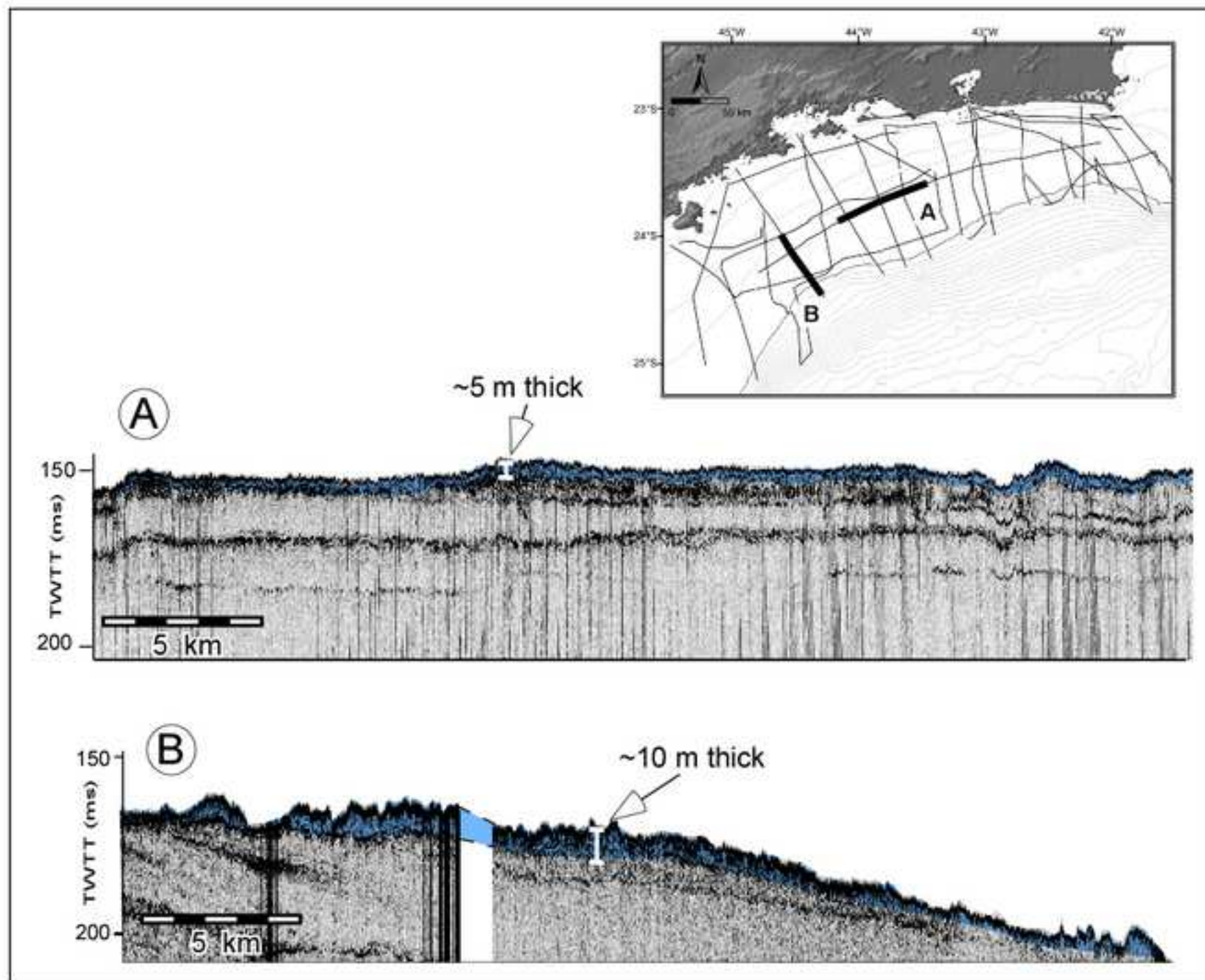
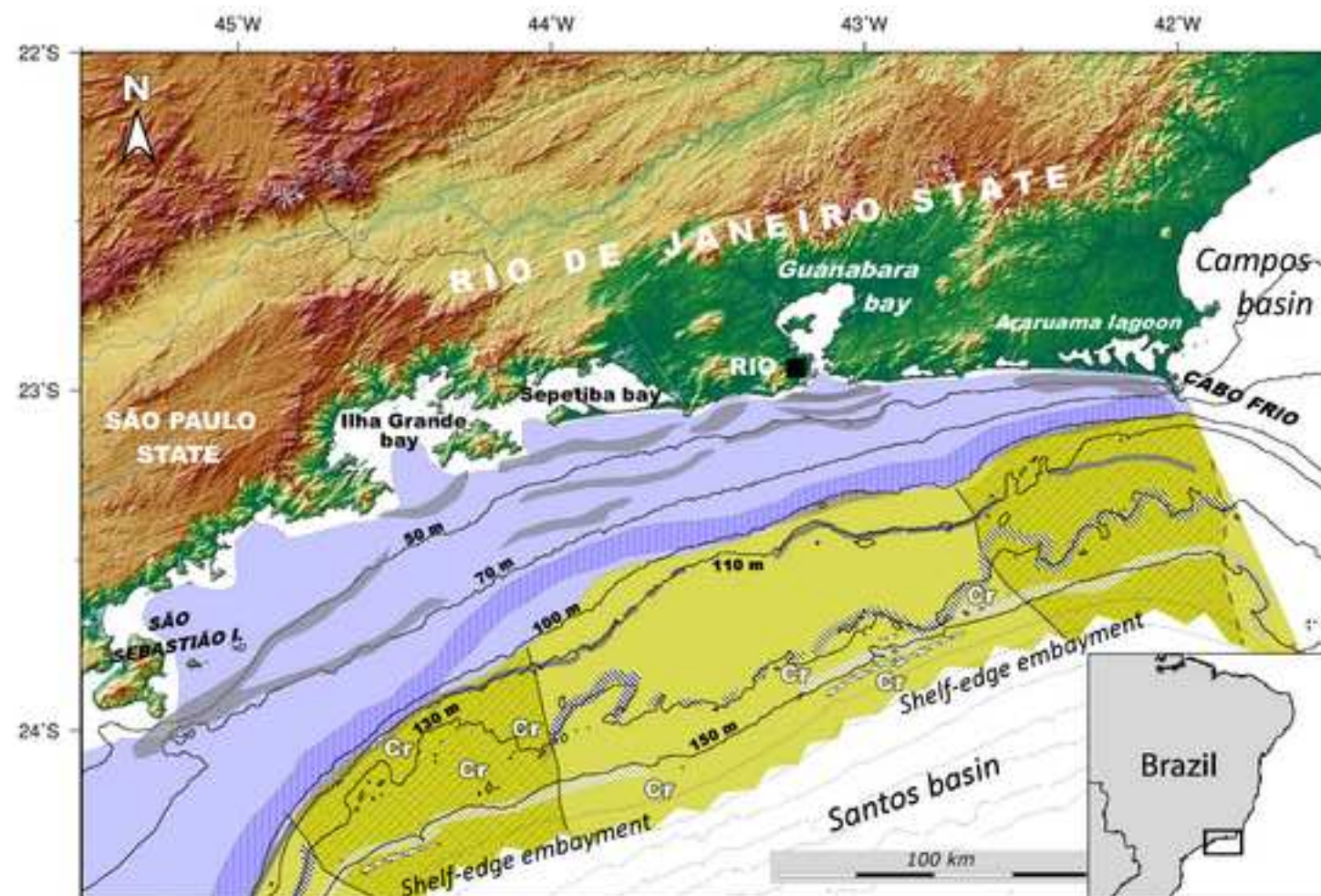


Figure15

[Click here to download high resolution image](#)



LEGEND











- | | | | |
|---|--|---|---|
|  | Escarpment imprinted by downstepping forced-regressive Sq4 wedges |  | Main zones of erosion and sediment bypass |
|  | Escarpment imprinted by wave-cut erosion during the LGM |  | Regional lobate sea-floor morphology imprinted by Sq4 "highstand" deposition |
|  | Escarpment imprinted by the BC bottom erosion |  | Regional sea-floor morphology imprinted by Sq4 Falling-stage Systems Tract |
|  | Inclined steps imprinted by Sq4 transgressive-regressive wedges |  | Main occurrences of carbonate bioconstructions |
|  | Frontal foresets of Holocene prograding clinoforms or transgressive wedges |  | Channel at the foot of the -150 m scarp probably eroded by the intensified BC bottom currents along shelfbreak embayments |

Figure16
[Click here to download high resolution image](#)

